100 years later: new discoveries and observations on ceticolous diatoms

Authors: Frankovich, Thomas A., Majewska, Roksana, Sullivan, Michael J., Huggins, Jessica L., Stepanek, Joshua G., et al.

Source: Proceedings of the Academy of Natural Sciences of Philadelphia, 169(1) : 49-78

Published By: The Academy of Natural Sciences of Philadelphia

URL: https://doi.org/10.1635/053.169.0105

ISSN 0097-3157

PROCEEDINGS OF THE ACADEMY OF NATURAL SCIENCES OF PHILADELPHIA 169: 49-77 2026

100 years later: new discoveries and observations on ceticolous diatoms

THOMAS A. FRANKOVICH*

Florida International University, Florida Bay Interagency Science Center, 98630 Overseas Highway, Key Largo, FL 33037 USA
E-mail: tfrankov@fiu.edu

ROKSANA MAJEWSKA

Faculty of Biosciences and Aquaculture, Nord University, Postboks 1490, 8049 Bodø, Norway
Biomedical and Molecular Metabolism Research (BioMMet), Faculty of Natural and Agricultural Sciences, North-West University, Private Bag X6001, Potchefstroom 2520, South Africa
E-mail: roksana.majewska@nord.no

MICHAEL J. SULLIVAN

130 Martinique Drive, Madison, MS 39110 USA
E-mail:diatomman@hotmail.com

JESSICA L. HUGGINS

Cascadia Research Collective, 218 ½ W 4th Ave, Olympia, WA 98501 USA
E-mail: jhuggins@cascadiaresearch.org

JOSHUA G. STEPANEK

Colorado Mountain College Vail Valley, 150 Miller Ranch Road, Edwards, CO 81632 USA
E-mail: jstepanek@coloradomtn.edu

MATT P. ASHWORTH

UTEX Culture Collection of Algae, Department of Molecular Biosciences, University of Texas, Austin, 205 W. 24th St., Biological Sciences Building, Austin, TX, 78712 USA
E-mail: mashworth@utexas.edu

RANDALL S. WELLS

Sarasota Dolphin Research Program, Brookfield Zoo Chicago, c/o Mote Marine Laboratory, 1600 Ken Thompson Parkway, Sarasota, FL, 34236 USA
E-mail: rwells@mote.org

ABSTRACT.— Biofilms from the skin of ten cetacean species and from the baleen of gray, humpback, and common minke whales were examined for ceticolous diatoms. Two new epizoic diatoms, *Tursiocola cymbelloides* sp. nov. and *Halamphora baleenicola* sp. nov. were described from baleen of gray whales (*Eschrichtius robustus*) and a humpback whale (*Megaptera novaeangliae*), respectively. New ultrastructure details are also described of the rarely observed ceticolous diatoms *Epiphalaina aleutica*, *Tursiocola staurolineata*, *Plumosigma rimosum*, *Bennettella ceticola*, and *Epipellis heptunei*. A newly named structure, the "solea", associated with the polar raphe endings of *P. rimosum* is described in detail, as is a rudimentary butterfly structure in *E. aleutica* that further blurs the distinctions between the diatom genera *Epiphalaina* and *Tursiocola*. This study also adds four cetacean species to the relatively short list of cetaceans examined microscopically for diatoms.

Keywords: epizoic diatoms, biofilm, whales, cetaceans, new species, SEM

* Corresponding author

Submitted: 19 July 2025, Accepted 22 Oct 2025.

INTRODUCTION

Marine megafauna have an especially unique diatom flora on their body surfaces (Nemoto, 1956; Holmes et al., 1993a, 1993b; Majewska et al., 2020). The diatom assemblages consist of incidental free-living taxa, often in low relative abundance, that settle onto the animals from the surrounding environment, but more interestingly, a core group of obligately epizoic species often dominates (Majewska et al., 2020, 2021; Azari et al., 2020; Ashworth et al., 2022). The association of diatoms with their various hosts has driven the diversification of both new species (Denys, 1997; Frankovich et al., 2015; Riaux-Gobin et al., 2017) and novel traits including obligate heterotrophy (Frankovich et al., 2018). The composition of these core epizoic diatom assemblages extends beyond the species level and includes specialized genera such as *Bennettella* R.W.Holmes 1985, *Plumosigma* T.Nemoto 1956, *Tursiocola* R.W.Holmes, S.Nagasawa and H.Takano 1993, *Epiphalaina* R.W.Holmes, S.Nagasawa and H.Takano 1993, *Epipellis* Holmes 1985, *Tripterion* R.W.Holmes, S.Nagasawa and H.Takano 1993, and *Medlinella* Frankovich, Ashworth and M.J.Sullivan 2016 that are only known from the epizoic habitat.

Despite over 100 years since the first publication reporting on the microscopic examination and taxonomy of ceticolous diatoms (Bennett, 1920), epizoic diatom diversity and their distribution on cetacean species remains far from complete. Only 25 of the 94 presently known cetacean species have been examined microscopically for epizoic diatoms (Table 1). The challenges that limit investigation are significant and match those that inhibit studies on the animals themselves. Many cetaceans remain endangered and require special and restrictive permits to study. The large size and pelagic habitat of many whales and dolphins preclude most live captures that can be harmful for both the animals and researchers. Recent investigations have been reliant on infrequent mortality events or rare strandings to obtain skin scrapings from these animals (Denys, 1997; Ferrario et al., 2019). When stranded animals are available for study, the condition of the animals may not be suitable for preservation of epizoic diatoms because of putrefaction or scouring if the animal strands in heavy surf. If the body is in good condition, successful examination of the microflora may still be difficult because epizoic diatom distribution on the animal is often patchy and sporadic (Holmes et al., 1993a), or hidden by dark skin color (Bennett, 1920). Diatom colonies were only observed on 2% of over 1000 Dall's porpoises examined at a wholesale fish market (Holmes et al., 1993a). It is fair to say that examination of epizoic diatoms on cetaceans is difficult and infrequent.

Twenty diatom taxa are known only from the epizoic habitat on cetaceans (Table 2). Of those, *Bennettella ceticola* (E.W.Nelson) R.W.Holmes 1985, *B. constricta* (T.Nemoto) R.W.Holmes 1985, *Epipellis oiketis* R.W.Holmes 1985, *Epiphalaina aleutica* (T.Nemoto) R.W.Holmes, S.Nagasawa and H.Takano 1993, and *Tursiocola olympica* (Hustedt) R.W.Holmes, S.Nagasawa and H.Takano 1993 are the most frequently reported species and six taxa have not been reported or studied since they were first described (Table 2). Most diatomists may not be familiar with the obligately epizoic genera as descriptions of these genera were not included in Round et al. (1990), the major reference book surveying the diatom genera. To assist those not specializing in epizoic diatoms, a guide to the epizoic diatom literature on cetaceans is provided in Table 2 and the following diagnostic key to the six obligately epizoic diatom genera on cetaceans is presented.

Diagnostic key to obligately epizoic diatom genera occurring on cetaceans

1. Frustules heterovalvar, cells adnate, valves elliptical....2

- Frustules isovalvar.....3

2. External distal raphe ends obscured by silica flap.....*Bennettella*

- External distal raphe ends not obscured.....*Epipellis*

3. Frustules strongly heteropolar with distinct head and foot poles.....*Tripterion*

- Frustules isopolar or indistinctly heteropolar.....4

4. Valves sigmoid.....*Plumosigma*

- Valve outline otherwise.....5

5. Valves with distinct "butterfly structure" at internal central area.....*Tursiocola*

- "Butterfly structure" lacking or incompletely developed.....*Epiphalaina*

The objectives of this paper are to describe two new species of ceticolous diatoms and provide new ultrastructural details of *Epiphalaina aleutica*, *Plumosigma rimosum* T.Nemoto 1956, *Bennettella ceticola*, *Epipellis heptunei* Denys and Van Bonn 2001, and *Tursiocola staurolineata* Denys 1997. The above-mentioned established species of epizoic diatoms, due

Table 1. Cetacean species that have been examined microscopically for epizoic diatoms. References: 1 – Bennett, 1920, 2 – Denys, 1997, 3 - Denys and De Smet, 2010, 4 – Denys and Van Bonn, 2001, 5 – Ferrario et al. 2019, 6 – Gerasimiuk and Zinchenko, 2012, 7– Goldin, 2010, 8 – Hart, 1935, 9 – Holmes, 1985, 10 - Holmes et al. 1989, 11 - Holmes et al. 1993a, 12 - Holmes et al. 1993b, 13 – Holmes and Nagasawa, 1995, 14 – Hustedt, 1952, 15 – Kliashtorin, 1962, 16 – Morejohn, 1980, 17 – Nemoto, 1956, 18 – Nemoto, 1958, 19 – Nemoto et al. 1977, 20 – Nemoto et al. 1980, 21 – Okuno, 1954, 22 – Omura, 1950.

	References
Balaenidae	
Eubalaena australis, southern right whale	8
Eubalaena glacialis, northern right whale	15
Balaenopteridae	
Balaenoptera bonaerensis, Antarctic minke whale	6
B. borealis, sei whale	8, 15, 17
B. acutorostrata, common minke whale	9, 20, present study
B. musculus, blue whale	1, 8, 9, 17, 18, 22
B. physalis, fin whale	1, 8, 9, 17, 21, 22, present study
B. ricei, Rice's whale	present study
Eschrichtius robustus, gray whale	15, present study
Megaptera novaeangliae, humpback whale	8, 9, 14, 17, present study
Delphinidae	
Lagenorhyncus obliquidens, Pacific white-sided dolphin	16
Orcinus orca, killer whale	9, 12, 15, 20
Pseudorca crassidens, false killer whale	present study
Stenella coeruleoalba, striped dolphin	16
Tursiops truncatus, bottlenose dolphin	4, 7,present study
Kogiidae	
Kogia sp., pygmy/dwarf sperm whale	present study
Phocoenidae	
Phocoenoides dalli, Dall's porpoise	9, 10, 11, 16
Phocoena phocoena, harbor porpoise	3, 16, present study
Physeteridae	
Physeter macrocephalus, sperm whale	2, 8, 13, 15, 17, present study
Pontoporiidae	
Pontoporia blainvillei, La Plata dolphin	5, 19
Ziphiidae	
Berardius bairdii, Baird's beaked whale	13, 15, 19
Hyperoodon planifrons, southern bottlenose whale	5, 13, 20
Mesoplodon europaeus, Gervais's beaked whale	present study
Mesoplodon layardii, strap-toothed whale	12, 20
Ziphius cavirostris, Cuvier's beaked whale	13, 18

Table 2. Putative obligately-epizoic diatom taxa on cetaceans. References: 1 – Bennett (1920), 2 – Denys (1997), 3 - Denys and De Smet (2010), 4 – Denys and Van Bonn (2001), 5 – Ferrario et al. (2019), 6 – Frankovich et al. (2016), 7 – Gerasimiuk and Zinchenko (2012), 8 – Hart (1935), 9 – Holmes (1985), 10 – Holmes et al. (1989), 11 – Holmes et al. (1993a), 12 – Holmes et al. (1993b), 13 – Holmes and Nagasawa (1995), 14 – Hustedt (1952), 15 – Kliashtorin (1962), 16 – Morejohn (1980), 17 – Nemoto (1956), 18 – Nemoto (1958), 19 – Nemoto et al. (1977), 20 – Nemoto et al. (1980), 21 – Okuno (1954), 22 – Omura (1950), 23 – Proschkina-Lavrenko (1961), 24 – Usachev (1940), 25 – present study.

Taxon	Synonyms	References
Bennettella ceticola (E.W. Nelson) R.W.Holmes	*Cocconeis ceticola* E.W.Nelson *C. ceticola* f. *ovalis* (nomen nudum) *C. ceticola* f. *subconstricta* T.Nemoto *C. ceticola* var. *arctica* Usachev	1, 5, 7–10, 16–22, 24, 25
B. constricta (T.Nemoto) R.W.Holmes	*Cocconeis ceticola* f. *constricta* T.Nemoto *C. ceticola* f. *berardii* L.B.Kliashtorin *Bennettella berardii* R.W.Holmes & S.Nagasawa	9, 13, 15, 17, 20
Cocconeis ceticola var. *subsalina* Proschkina-Lavrenko		23
C. costata var. *pacifica* f. plana T.Nemoto		17
Epipellis heptunei L.Denys and W.Van Bonn		4, 25
E. oiketis R.W.Holmes	*Cocconeis ceticola* f. *suborbicularis* (nomen nudum) *C. orcii* (nomen nudum)	3, 9, 10, 15, 16
Epiphalaina aleutica (T.Nemoto) R.W.Holmes, S.Nagasawa and Takano	*Stauroneis aleutica* T.Nemoto *Epiphalaina aleutica* var. *lineata* Denys	2, 10, 11, 17, 25
E. radiata R.W.Holmes, S.Nagasawa and Takano		12, 20
Gomphonema hartii T.Nemoto		17
Halamphora baleenicola sp. nov.		25
Licmophora onassisii Hustedt		14
Plumosigma hustedtii T.Nemoto		17
P. rimosum T.Nemoto		17, 25
Stauroneis aleutica f. *brevis* T.Nemoto		17
Tripterion kalamensis R.W.Holmes, S.Nagasawa and Takano		6, 11
T. philoderma R.W.Holmes, S.Nagasawa and Takano		6, 12
Tursiocola cymbelloides sp. nov.		25
T. olympica (Hustedt) R.W.Holmes, S.Nagasawa and Takano	*Stauroneis olympica* Hustedt	2, 11, 14, 17, 20
T. omurae (T.Nemoto) R.W.Holmes, S.Nagasawa and Takano	*Stauroneis omurae* T.Nemoto	2, 17
*T. staurolineat*a L.Denys		2, 10, 11, 25

to their unique habitat, are rarely encountered, reported, and documented. We also report on the examination of biofilms sampled from live and stranded animals and from museum specimens. The examined biofilms were from the skin of ten cetacean species and from the baleen of gray, humpback, and common minke whales (Table 1).

MATERIAL AND METHODS

Diatom methodology.—Diatoms were examined from the skin and baleen of recently deceased and stranded cetaceans, from dried whale skin museum specimens obtained from the Canadian Museum of Nature, and from the skin of live bottlenose dolphins sampled as part of the Sarasota Dolphin Research Program, a capture-release veterinary research program (Wells et al., 2004). Toothbrushes were used to collect biofilm from various locations on the body surfaces. Separate toothbrushes were used for each individual and body location. The biofilm collected onto the toothbrushes was rinsed into 20-ml sample bottles with ambient water for further morphological examinations. Following observations for any live specimens, samples were oxidized in boiling 30% nitric acid followed by addition of potassium dichromate (approximately 150 mg per sample). Cleaned diatoms were settled from the suspension for a minimum of 6 h, and the remaining acid solution was decanted. The settled diatoms were rinsed with deionized water and settled again. The rinsing/settling/decanting process was repeated six times.

Museum specimens of dried whale skin were either digested in a mixture of boiling concentrated acids according to von Stosch's method (small and damaged samples; Hasle and Syvertsen, 1997) or immersed in distilled water and sonicated, depending on the state and size of the available skin sample. The diatom suspension in distilled water was subsequently centrifuged to concentrate the diatom material, treated with acids to remove any organic matter still present in the samples, centrifuged, and rinsed thoroughly with distilled water (Majewska et al., 2018). Light microscopy (LM) analyses were made using a Nikon E600 microscope equipped with differential interference contrast (DIC), and 40× Nikon Plan Fluor (NA = 0.75) and 60× oil immersion Nikon Plan Apo (NA = 1.40) objectives for observing live and cleaned specimens, respectively. For LM examination of cleaned specimens, diatoms were air-dried on No. 1.5 coverslips, which were then mounted onto glass slides using Naphrax. Photomicrographs were produced using a Leica DFC425 digital camera and measurements of diatom characters were produced using Leica Application Suite imaging software version 3.7. For scanning electron microscopy (SEM), subsamples of the cleaned material were dried onto aluminum stubs and sputter-coated with gold/palladium or iridium to a thickness of 1 nm. SEM analyses were made with a JEOL-5900LV scanning electron microscope operated at 20 kV and a Zeiss SUPRA 40 VP scanning electron microscope operated at 7 kV, or a FEI Quanta FEG 250 scanning electron microscope operated at 15kV and 20kV, and a JEOL JSM-7001F scanning electron microscope operated at 5 kV.

Relative abundances of individual taxa were determined from the holotype slides of the new species by identifying and counting 506–540 diatom valves along arbitrary linear transects. Diatom terminology follows Anonymous (1975), Ross and Sims (1972), Round et al. (1990), Denys (1997), and Majewska (2020). The use of the morphological term "stauros" follows Cox (2012). The morphological term "butterfly structure" is a specialized term that is not encountered outside of the study of epizoic diatoms and previously has been unique to the genus *Tursiocola*. Because most readers will not be familiar with the term, we define the term as an extension of the pseudosepta that run along the lateral margins of the valve and then extend towards the central area merging with the stauros often forming a roofed structure. Readers are referred to Majewska (2020) for a discussion of the butterfly structure and questions regarding its relationship to the stauros and pseudosepta.

Host sampling methodology - stranded cetaceans.—Biofilm was collected from 21 deceased and stranded cetaceans representing 8 species (Table 3). Further details about the gray and humpback whales that yielded specimens used for the new diatom species descriptions are provided below.

On July 6 2019, a dead gray whale, *Eschrichtius robustus,* (animal identification number CRC-1740) was found floating in Budd Inlet in southern Puget Sound, Washington, U.S.A (King 5 Staff, 2019). The carcass was towed to a secure location and a necropsy was conducted on July 7. Biofilm samples obtained during the necropsy include sample number W02 (baleen) that was used to describe *Tursiocola cymbelloides* sp. nov. (described later in the Results).

On May 19 2020, a dead gray whale (animal identification number WDFW2020-055) washed ashore near Manitou Beach in Puget Sound, Washington, U.S.A (Reicher, 2020). Biofilm samples obtained during the necropsy on May 20 include sample number W08 (baleen) used to describe *Tursiocola cymbelloides* sp. nov.

On July 26 2020, a humpback whale, *Megaptera novaeangliae,* (animal identification number CRC-1816) washed ashore dead in Ocean Shores, Washington, U.S.A. (King 5 Staff 2020). Biofilm samples were obtained during

the necropsy on July 27. The baleen biofilm (sample number W35) contained an abundance of *Halamphora baleenicola* sp. nov. and *Tursiocola cymbelloides* sp. nov. described later in the Results.

Host sampling methodology - museum specimens.—Dried whale skin from fin whale (*Balaenoptera physalis*) and sperm whale [*Physeter macrocephalus* (as *Physeter catadon*)] specimens were obtained from the Canadian Museum of Nature. The following specimens were examined—Fin whale: CANA 12661, CMNMA 57071, CMNMA 58783, CANA 126267, CANA 126260, CANA 126261, CMNMA 57963, CMNMA 58673, CMNMA 58686, and CMNMA 58721;—Sperm whale: CANA 126264, CANA 126273, CMNMA 59235, CMNMA 59236, CMNMA 59241, and CMNMA 59272. The whales were captured in the Canadian Arctic between 1967 and 1972; exact dates and location information of the specimens are unknown.

Host sampling methodology - live bottlenose dolphins.—17 skin biofilm samples were collected from nine bottlenose dolphins during brief catch-and-release health assessments of long-term resident dolphins in Sarasota Bay, Florida (27° 23' N, 82° 35') during May 8–12, 2017. The dolphins were encircled with a 500-m-long seine net in shallow water and handled and sampled as described by Wells et al. (2004). The animal identification numbers of the sampled dolphins are F151, F164, F173, F242, F263, F271, F296, F306, and F307. Biofilm was collected from various body locations including axilla ("armpit"), flippers, and back on the dorsal body surface.

Bottlenose dolphins were treated ethically and the study was carried out in strict accordance with the U.S. Marine Mammal Protection Act. Procedures for the dolphin catch-and-release operations were conducted under NOAA Fisheries Service Scientific Research Permit No. 20455 issued to Wells. Research was approved through the Mote Marine Laboratory annual Institutional Animal Care and Use Committee (IACUC) reviews. Stranding response activities were conducted under NOAA permit 18786-03. Research activities on marine mammal parts were conducted under NMFS permit 23802.

RESULTS

Stranded cetaceans.—Biofilm from stranded and deceased animals was examined from eight cetacean species (Table 3). Four of those species – *Pseudorca crassidens*, *Balaenoptera ricei*, *Kogia* sp., *Mesoplodon europaeus* – have not been examined microscopically for diatoms previously. The only epizoic diatom observed from the four newly examined cetacean species was a single frustule of an undescribed *Tursiocola* sp. from the skin of one of the false killer whales (*P. crassidens*). The single *Tursiocola* frustule found was insufficient for further study. The epizoic diatoms *Bennettella ceticola* and *Epipellis oiketis* were observed in the skin biofilm from the three harbor porpoises (*Phocoena phocoena*) examined. *Bennettella ceticola* was abundant and the only diatom observed on two of those porpoises, while the third porpoise harbored a sparse assemblage of both species. The skin biofilm from the examined gray whales (*Eschrichtius robustus*) had scarce incidental diatoms from the plankton and benthos but the baleen had an abundance of *Tursiocola cymbelloides* sp. nov. (described below). The baleen from the humpback whale (*Megaptera novaeangliae*) stranded on the Washington coast had an abundance of *T. cymbelloides* and *Halamphora baleenicola* sp. nov. (described below), while the skin biofilm was mostly devoid of diatoms (Table 3). Biofilms sampled from the skin and baleen of the humpback whale stranded on the New Jersey coast contained only sparse planktonic and psammophilic diatoms (Table 3) assumed to originate from the stranding site. Only incidental diatoms from the plankton and benthos were observed in the skin and baleen biofilms from the common minke whale stranded in Washington.

Live bottlenose dolphins.—Diatoms were observed in the skin biofilm from 8 of the 9 dolphins but abundances were very sparse in all of the samples and consisted almost entirely of the epizoic diatom *Epipellis heptunei* (described later in the Results). Incidental diatoms from the plankton or benthos were not observed, except for one valve of the benthic centric diatom *Mastodiscus radiatus*. A single valve of an undetermined *Tursiocola/Epiphalaina* species was also recorded. Descriptions of *E. heptunei* were produced from skin biofilm sampled from the left axilla of dolphin F296 and from the left flipper of dolphin F151.

Diatom descriptions

***Tursiocola cymbelloides* Frankovich, Ashworth and M.J. Sullivan sp. nov.**

Figures 1–33

Description.—LM morphology: Frustules rectangular in girdle view with bluntly rounded poles (Figs. 1–5). Valves strongly dorsiventral. Valve face outline narrowly semi-lanceolate (Figs. 9–14) to broadly semi-lanceolate (Figs. 6–8), dorsal margin convex, ventral margin straight (Figs. 6–14). Valve apices acute (Figs. 6–14). Valve morphometrics: length 21–35 μm, width 1.6–3.7 μm, length

Table 3. Collection information of the cetaceans sampled for diatoms.

Date	Cetacean species	Identification number	Stranding location	Latitude and Longitude	Diatom observations and comments
May 1 2013	*Phocoena phocoena*, harbor porpoise	CRC-1252	Puget Sound, Seattle, Washington, U.S.A.	47° 34' N, 122° 25' W	*Bennettella ceticola* was abundant and the only diatom observed in the skin biofilm.
January 19 2017	*Pseudorca crassidens*, false killer whales	Not available	Hog Key, Everglades National Park, Florida, U.S.A.	25° 34' N, 81° 14' W	One valve of *Auliscus* sp. and one frustule of an undescribed *Tursiocola* sp. was obtained from the skin biofilms from 10 carcasses.
January 31 2019	*Balaenoptera ricei*, Rice's whale	Not available	Sandy Key, Everglades National Park, Florida, U.S.A.	25° 02' N, 81° 01' W	Only incidental benthic diatoms familiar to Florida Bay (e.g., *Mastogloia* spp., *Cocconeis* spp.) were observed from skin biofilm samples. Baleen was not sampled. Deceased animal was towed to shore through Florida Bay.
July 7 2019	*Eschrichtius robustus*, gray whale	CRC-1740	Budd Inlet, Washington, U.S.A.	47° 06' N, 122° 30' W	*Tursiocola cymbelloides* sp. nov. constituted >90% relative abundance in baleen biofilm. Further details provided in Results.
May 20 2020	*Eschrichtius robustus*, gray whale	WDFW2020-055	Bainbridge Island, Washington, U.S.A.	47° 39' N, 122° 54' W	Skin biofilm contained scarce incidental diatoms. Baleen biofilm contained an abundance of *Tursiocola cymbelloides* sp. nov. followed by incidental planktonic and benthic diatoms (e.g., *Thalassiosira* spp., *Paralia* sp., *Cocconeis* spp.). Further details provided in Results.
July 27 2020	*Megaptera novaeangliae*, humpback whale	CRC-1816	Ocean Shores, Washington, U.S.A.	46° 56' N, 124° 10' W	Only 2 assumed incidental pennate diatom valves observed from the skin biofilm. The baleen biofilm contained an abundance of *Halamphora baleenicola* sp. nov. and *Tursiocola cymbelloides* sp. nov. described later in the Results.
September 8 2020	*Phocoena phocoena*, harbor porpoise	WDFW2020-151	Kingston, Washington, U.S.A.	47° 49' N, 122° 29' W	*Bennettella ceticola* was abundant and the only diatom observed in the skin biofilm.
December 11 2020	*Phocoena phocoena*, harbor porpoise	EJC-2020-33	Sequim, Washington, U.S.A.	48° 07' N, 123° 05' W	*Epipellis oiketis* and *Bennettella ceticola* were sparse and the only diatoms observed in the sample.
December 28 2020	*Megaptera novaeangliae*, humpback whale	MMSC-20-160	Barnegat Light, New Jersey, U.S.A.	39° 45' N, 74° 06' W	Only sparse incidental planktonic (e.g., *Thalassiosira aestivalis, T. angulata*) and psammophilic diatoms (e.g., *Anorthoneis hyalina, Psammodictyon* sp., *Amphicocconeis disculoides*) were observed in the skin and baleen biofilms.
March 17 2022	*Kogia* sp., dwarf sperm whale	Not available	Key Largo, Florida, U.S.A.	25° 05' N, 80° 26' W	Biofilm was brushed from the skin and teeth but no diatoms were observed.
October 7 2022	*Balaenoptera acutorostrata*, common minke whale	2022-SJ03	Lopez Island, Washington, U.S.A.	48° 35' N, 122° 45' W	Only incidental diatoms from the plankton and benthos observed in the skin and baleen biofilms.
August 14 2023	*Mesoplodon europaeus*, Gervais's beaked whale	Not available	Tavernier, Florida, U.S.A.	25° 01' N, 80° 28' W	Examination of skin biofilm samples yielded no diatoms.

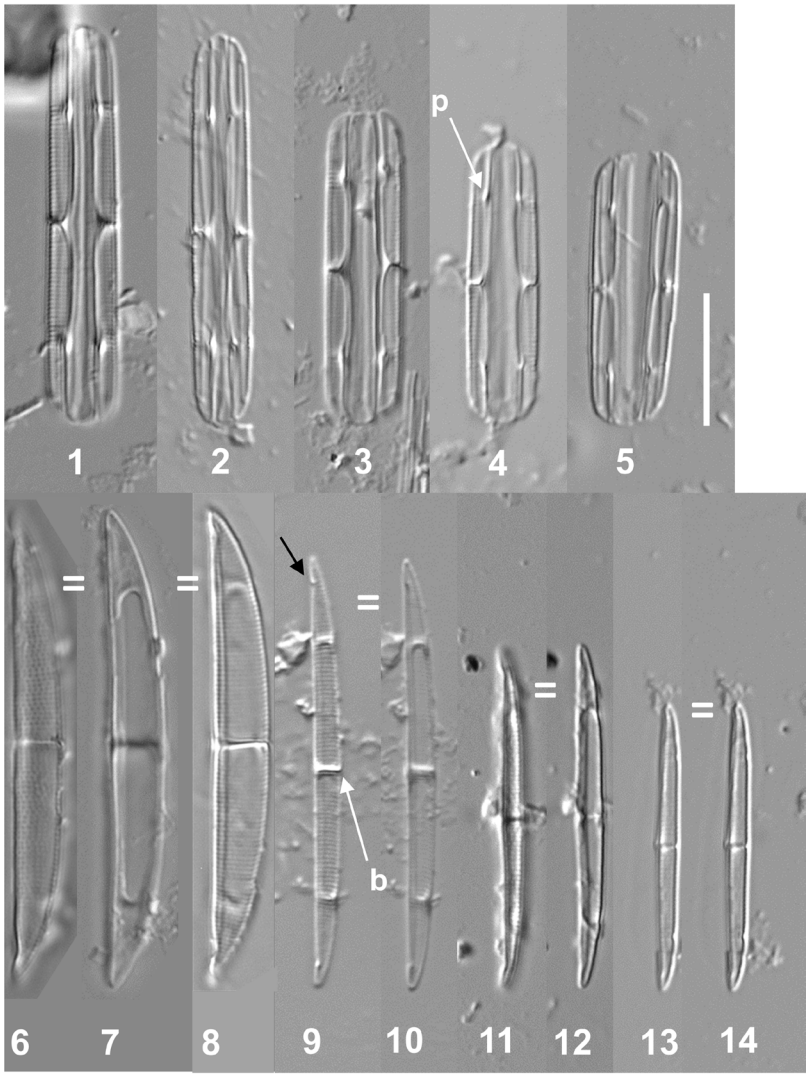

Figs. 1–14: (above) *Tursiocola cymbelloides* sp. nov. Type population, LM. Figs. 1–5, Frustules in girdle view showing size range and morphological variation. Pseudosepta (p) evident extending from valve apices. Figs. 6–14, Valves in valve view showing size range and morphological variation. Butterfly structure (b) evident as transapical line at valve middle. Thickened polar raphe endings (black arrow) evident short distance from apices near ventral margin. Scale bar: Figs. 1–14 = 10 μm. = indicates same specimen photographed at different focal planes.

Figs. 15–25: (page 57) *Tursiocola cymbelloides* sp. nov. Type population, SEM, external views. Fig. 15, Entire frustule in ventral girdle view showing cingulum with multiple copulae, deflected polar raphe endings (arrowhead) and areas of shortened striae on the valve mantle (arrow). Fig. 16, Entire frustule in dorsal girdle view showing areas of shortened striae on the valve mantle (arrows). Fig. 17, Detail of valve central area, conopeum (c), attached copulae and middle tab (t) on valvocopula. Fig. 18, Valve with semi-lanceolate valve outline. Fig. 19, Valve with linear semi-lanceolate valve outline. Fig. 20, Detail of valve apex showing polar raphe ending terminating short distance from apex. Fig. 21, Valve showing raphe strongly displaced towards ventral margin. Fig. 22, Dorsal side view of valve. Fig. 23, Detached cingulum showing middle tabs (t) on valvocopulae. Fig. 24, Detail of middle tab (t) on pars interior of valvocopula. Upper part of micrograph depicts fractured valve with cross-section of the butterfly structure (b). Fig. 25, Detail of cingulum construction at apex showing closed valvocopula (vc) and open abvalvar copulae (c1–c5) of epicingulum. Scale bars: Figs. 15–16, 18–19, 21–23 = 10 μm; Figs. 17, 20, 24–25 = 1 μm.

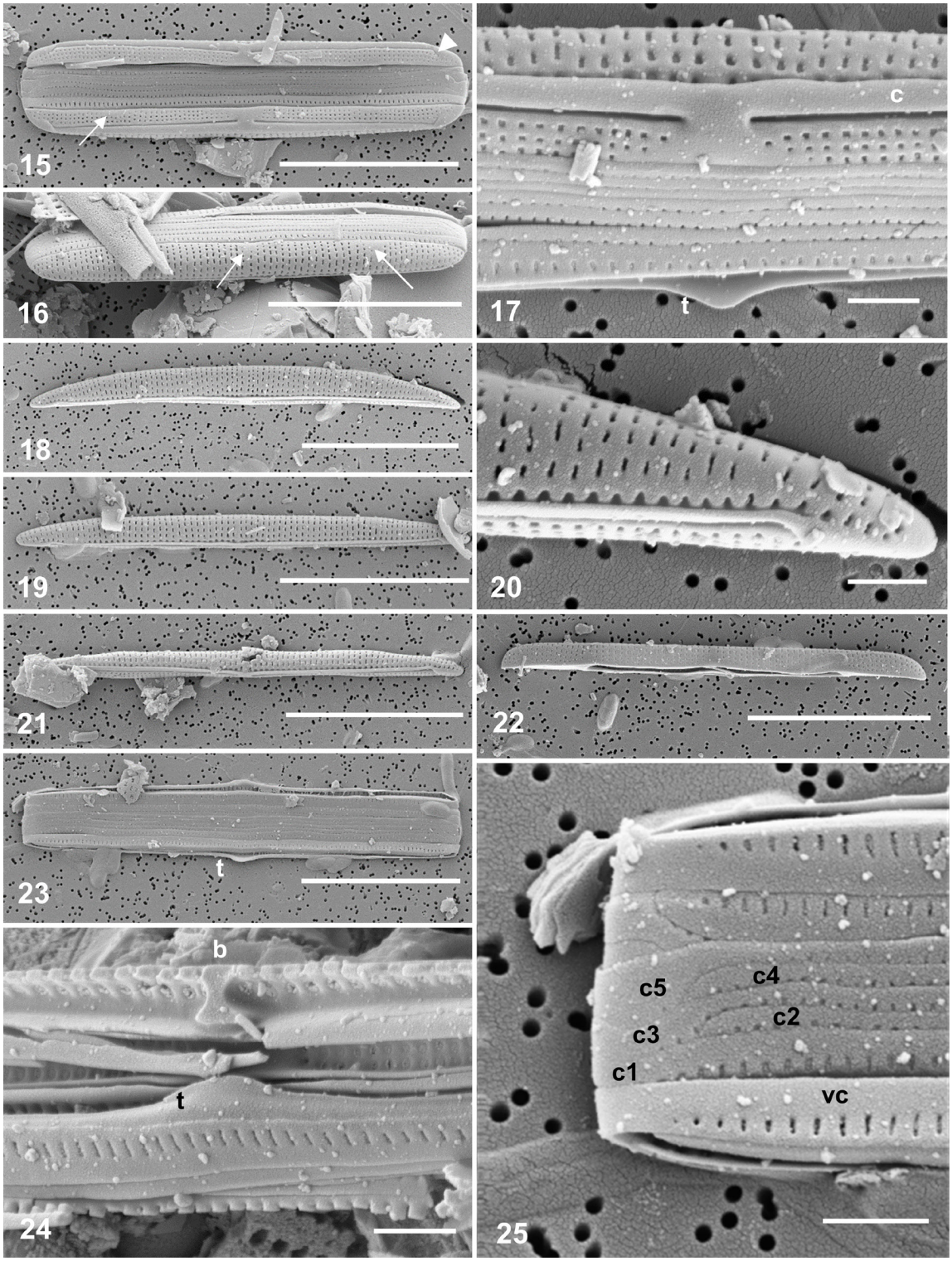

to width ratio 11–17, n > 470. Raphe barely discernible on ventral margin of larger frustules in ventral girdle view (Figs. 2, 4–5). Helictoglossae a short distance from valve apices, evident in frustule girdle views (Figs. 2–5). A diagonal flap of thickened silica poleward of the ventrally deflected polar raphe endings presenting a false appearance of ventrally deflected apices (Figs. 6–14). Unornamented triangular central area at middle of ventral margin evident in frustule girdle view (Figs. 1, 3). Transapical striae on valve face and mantle barely discernible, nearly parallel in the middle of the valve becoming slightly radiate towards apices (Figs. 6, 8–9). Internal butterfly structure apparent in girdle and valve views as a narrow refractive line across valve middle (Figs. 1–14). Pseudosepta evident in girdle and valve views (Figs. 1–5, 7–14). Pseudosepta approximately 1/5 of valve length from each apex (Figs. 1–5, 7–10, 12–14) connecting to narrow strips along valve margin (Fig. 7).

SEM morphology: Externally, dorsal portion of valve face with uniseriate transapical striae, 29–32 in 10 μm, n = 17. Striae composed of transapically elongated areolae with irregular outlines (Figs. 16–21, 27). Areola density approximately 35 in 10 μm. Two middle striae more distantly spaced (Figs. 16–19, 21, 27). Ventral striae, 36–40 in 10 μm, n = 7, nearly parallel to slightly radiate throughout, consisting of 3–4 squarish areolae, approximately 40 in 10 μm, similar appearance to dorsal striae (Figs. 15, 17). Both dorsal and ventral striae shortened, not extending to valve margin at 1/5 of valve length from each apex and at valve middle (Figs. 15–17, 27, arrows). Moderately wide mantle (Fig. 22), without a break between valve face dorsal striae and mantle dorsal striae (Figs. 15–17). Fastigia absent at valve apices (Fig. 20). Raphe located on valve mantle (Fig. 15, 17–21), nearly straight descending only slightly towards the ventral margin at valve middle (Fig. 15). Axial area nearly non-existent on ventral side of valve (Figs. 15, 17, 20). Dorsal axial area consisting of the raphe-sternum extending into a narrow (approximately 0.5 μm) conopeum partially obscuring the raphe-adjacent areolae (Figs. 17, 20). Central raphe endings straight, simple (Fig. 17). Central area asymmetric, dorsal side undifferentiated from unornamented conopeum, ventral side an unornamented triangular area expanding towards the ventral margin (Figs. 15, 17). Terminal raphe fissures a short distance from the apices, deflected ventrally Figs. 15, 20–21).

Internally, areolae covered by hymenes (Fig. 26). Pseudosepta extending from the apices as unornamented plates that conceal internal apices and polar raphe endings (Figs. 27–30). Beyond polar region pseudosepta diverge into narrow strips along valve margins (Figs. 28–31, 33). At valve middle, narrow silica strips on dorsal margin widen and connect with the butterfly structure that is only present on dorsal side (Figs. 28–29, 31, 33). Internal raphe slit along center of raised siliceous rib (Figs. 24, 31–32), terminating at helictoglossae a short distance from apices (Fig. 32). Two rounded knob-like structures on rib on opposing sides of raphe at valve center (Figs. 31, arrow; 33).

Cingulum composed of closed valvocopulae (Figs. 23, 25, 30) and multiple open abvalvar copulae (Fig. 25). Valvocopulae are flanged inward on the pars interior (Figs. 23–25). The flange is widened at the valve middle into a pair of opposing tabs (Figs. 23–24). Valvocopulae ornamented with single row of pervalvarly elongated pores (Figs. 23–25), 38–43 in 10 μm. Though observation of individual abvalvar copulae was limited to overlapping bands within complete cingula, the copulae appear to be similarly ornamented to the valvocopulae, copula pore density = 47–55 in 10 μm.

Diagnosis.—The mantle position of the raphe of *Tursiocola cymbelloides* sets this species apart from any other in the genus and this characteristic should prevent misidentification of our new species. A cursory examination of separated valves using light microscopy may suggest the genus *Amphora* or *Medlinella* because of the valve outline, but simple focusing through the valve will reveal pseudosepta and the butterfly structure, which are also readily evident in complete frustules in girdle view and not found in species of either *Amphora* or *Medlinella*. The recently described *Tursiocola neliana* Majewska (Majewska, 2020) also exhibits a dorsiventral amphoroid valve morphology but its slightly eccentric raphe is readily evident and clearly situated on the valve face rather than the ventral mantle. *Tursiocola neliana* is also much smaller in length (8–21 μm). Frustules of *T. cymbelloides* observed in girdle view may be difficult to distinguish from other members of the genus, but careful focusing on the valve mantles on both sides of the frustule will reveal the raphe on one side of the frustule indicating *T. cymbelloides*.

Holotype.—Slide ANSP GC68071 made from the sample ANSP GCM6803 deposited in the Academy of Natural Sciences of Drexel University, Philadelphia, Pennsylvania USA.

Type locality.—Puget Sound, Washington USA (47° 06' 29" N, 122° 54' 38" W). Collected from the baleen of a stranded deceased gray whale *Eschrichtius robustus* by Jessie Huggins, 7 July 2019, diatom sample number W02.

Isotypes.—Slides BM 92454 deposited in the Natural History Museum, London, United Kingdom, and CANA 131861 deposited in the Canadian Museum of Nature, Ottawa, Ontario, Canada.

Etymology.—The specific epithet *cymbelloides* refers to the strongly dorsiventral organization of the valves about the apical plane as exemplified by the genus *Cymbella*, *-oides* (Greek) = -resembling.

Supplementary notes.—Taxa relative abundances on holotype slide: 25 taxa from 14 genera were observed in a count of 506 valves from the holotype slide ANSP GC68071. The newly described *Tursiocola cymbelloides* comprised 90.3% of the intact valves counted. Only an unidentified raphid diatom at 1.2% relative abundance constituted greater than 1.0% of the valve count. Apart from *T. cymbelloides*, other raphid diatoms comprised 7.5% of the diatom assemblage. Araphid planktonic diatoms - *Thalassionema*, *Rhizosolenia*, *Paralia*, *Cyclotella*, and *Thalassiosira* spp. - comprised 2.2% of the assemblage. Fragments of various frustules were abundant in the material. None of the other described *Tursiocola* or *Epiphalaina* taxa were observed in the material.

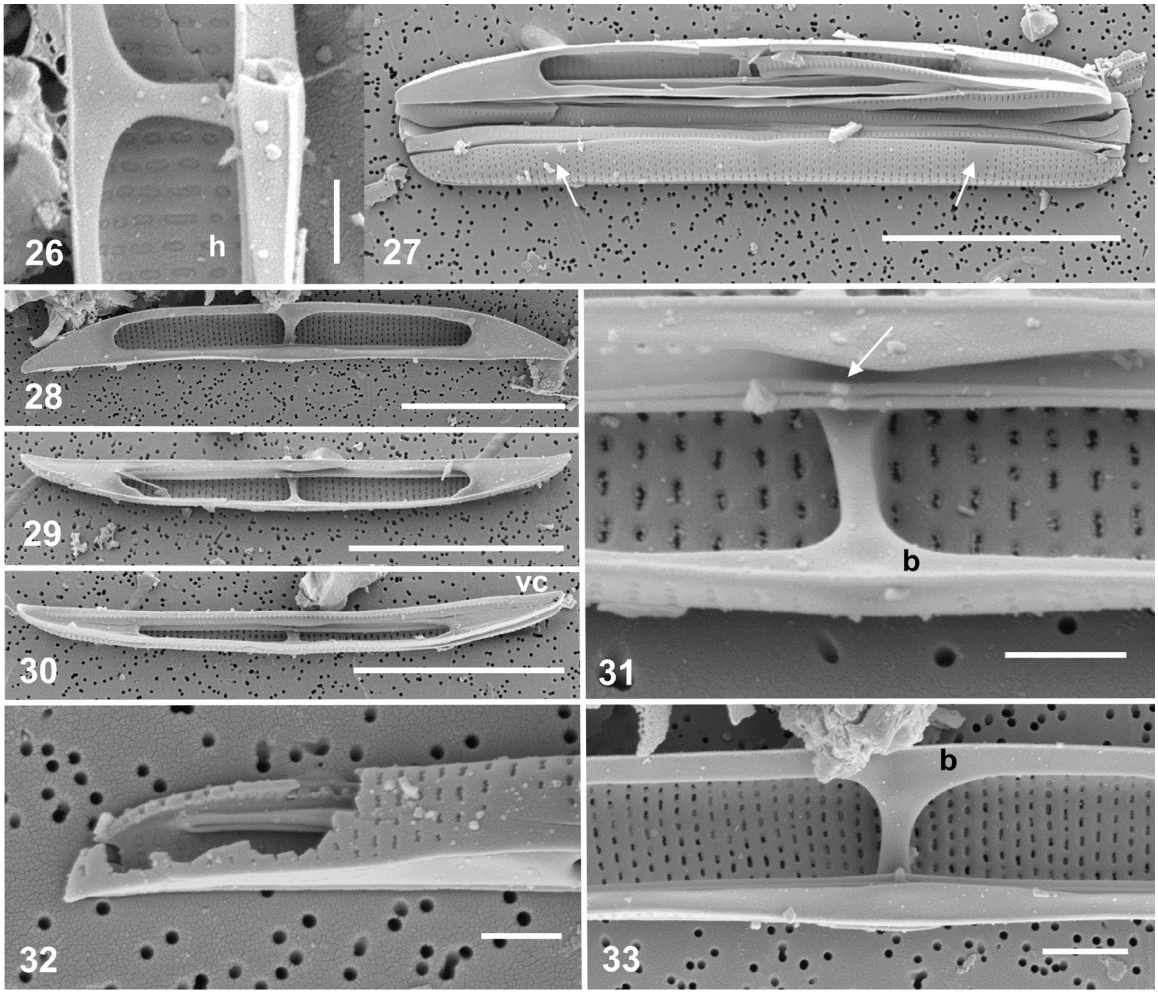

Figs. 26–33: *Tursiocola cymbelloides* sp. nov. Type population, SEM, internal views. Fig. 26, Detail of valve interior showing hymenate pore occlusions (h). Fig. 27, Frustule in dorsal girdle view with partially detached valve. Arrows indicate areas of shortened striae opposite termini of pseudosepta. Fig. 28, Valve showing extent of pseudosepta. Fig. 29, Oblique view of valve interior showing slight widening of pseudosepta at valve middle on ventral margin. Fig. 30, Oblique view of valve with attached valvocopula (vc). Fig. 31, Detail of butterfly structure (b) developed on dorsal side of valve and two knobs (arrow) on raised raphe ridge at valve center. Fig. 32, Partially broken valve apex revealing helictoglossa. Fig. 33, Detail of butterfly structure (b) and slightly widened pseudosepta on ventral margin opposite butterfly structure. Scale bars: Figs. 26, 31–33 = 1 μm; Figs. 27–30 = 10 μm.

***Tursiocola staurolineata* Denys 1997**
Figure 34

Description.—Frustules rectangular in girdle view, with bluntly rounded corners. Valves narrow, linear to narrowly lanceolate, very slightly heteropolar, with slender, acutely rounded apices. Length = 16–25 µm, width = 2.5–3.0 µm, length/width ratio 6.7–9.3, n = 20.

SEM morphology (Fig. 34)**:** Externally, valve face flat to slightly convex, connecting with a relatively shallow mantle without a clear transition. Valve edge slightly undulated. Striae uniseriate, parallel throughout most of the valve, becoming very slightly convergent close to the apices. Stria density: 31–35 in 10 μm, n = 12. Areolae nearly square to rounded. Axial area very narrow or indiscernible. Apices unornamented around polar raphe endings with one or two rows of areolae on valve mantle. Round central area expanded into a narrowing stauros reaching valve margins. Striae adjacent to the stauros slightly shortened. Raphe branches nearly straight and of slightly unequal length. Polar raphe endings unilaterally hooked, extending onto the valve mantle towards valve margin, with silica flaps expanding from primary side of valve and accentuating hooked shape of the structure. Central raphe endings straight, teardrop-shaped.

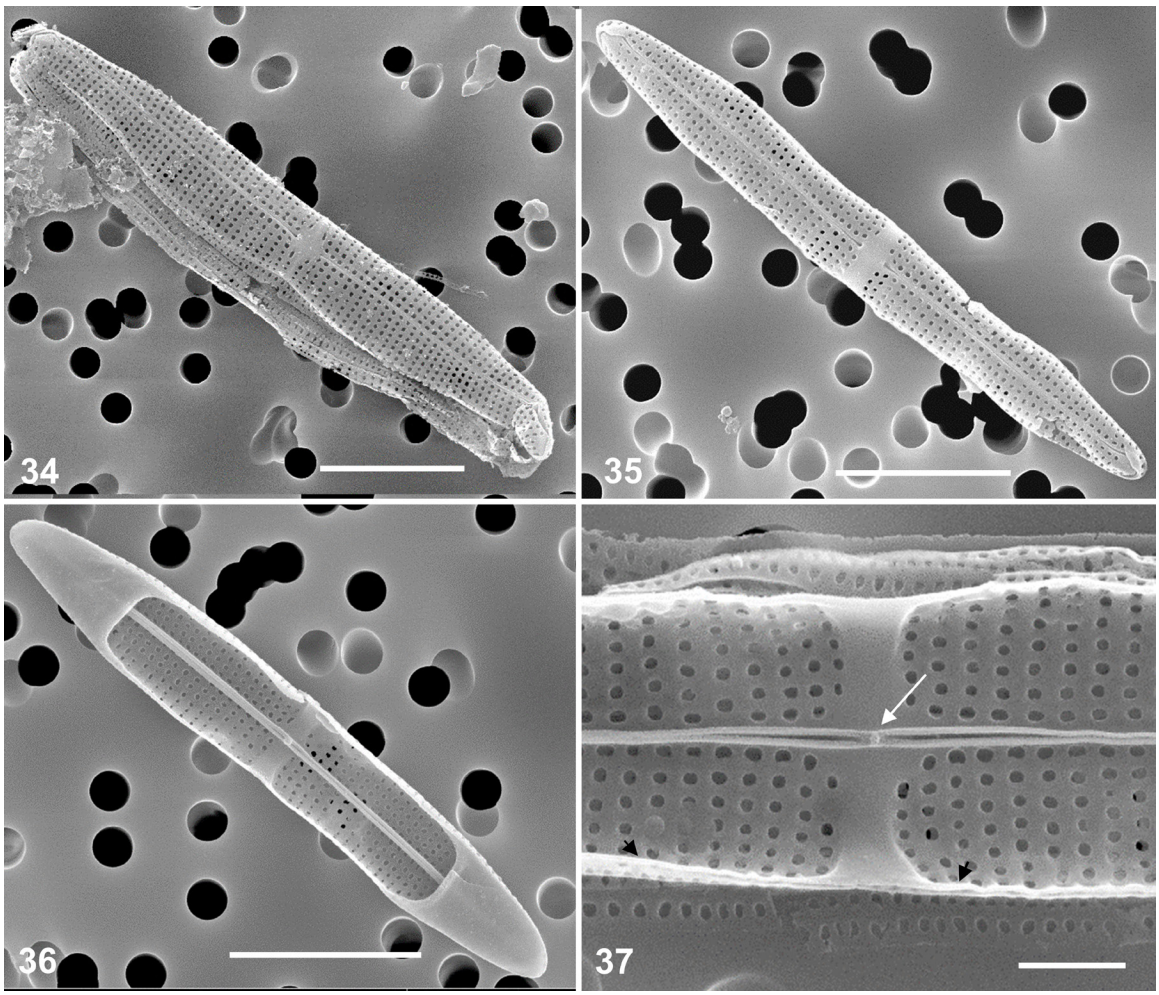

Figs. 34–37: *Tursiocola staurolineata* and *Epiphalaina aleutica*. SEM. Fig. 34, Frustule of *T. staurolineata* in oblique view. Fig. 35, Valve exterior of *E. aleutica* showing valve outline and rectangular stauros. Fig. 36, Valve interior of *E. aleutica* showing pseudosepta. Fig. 37, Detail of interior central area of *E. aleutica* showing internal raphe ridge, rudimentary butterfly structure, very narrow extensions of the pseudosepta (black arrowheads) and single knob (arrow) on raised raphe ridge. Scale bars: Figs. 34–36 = 5 µm; Fig. 37 = 1 µm.

Supplementary notes.—*Tursiocola staurolineata* was found in one museum specimen of dried whale skin obtained from the Canadian Museum of Nature, Ottawa, Canada. The sample was collected from the head area of a sperm whale (*Physeter catodon* [*P. macrocephalus*]; sample CMNMA 59235) caught in the Canadian Arctic in 1972. In that sample, *T. staurolineata* constituted 30.7% of the relative diatom abundance, and was accompanied by *Bennettella ceticola* (67%), *Plumosigma rimosum* (1.2%), and several other diatom taxa whose relative abundances did not exceed 0.1%.

Diagnosis.—*Tursiocola staurolineata* is most similar to *T. olympica* but differs in the structure of the external central area and the stauros (Denys, 1997; Frankovich et al. 2015). *T. staurolineata* has a small, round central area with a narrow stauros that decreases in width towards the mantle. *T. olympica* has a large, rectangular central area with a very broad, rhombic stauros.

Epiphalaina aleutica (T. Nemoto 1956) R.W. Holmes, S. Nagasawa and H. Takano 1993

Figures 35–37

Description.—Valves narrow, linear-lanceolate, very slightly heteropolar, with slender, acutely rounded apices that are demarcated from rest of the valve by pseudosepta. Length = 16–21 μm, width = 2.2–3.0 μm, length/width ratio 5.9–8.7, n = 25.

SEM morphology: Externally, valve face flat to slightly convex, connecting with a relatively shallow mantle without a clear transition. Valve margin straight. Striae uniseriate, parallel throughout most of the valve, becoming slightly convergent close to apices (Fig. 35). Stria density: 32–38 in 10 μm, n=12. Areolae nearly circular, internally occluded by hymenes. Axial area very narrow or indiscernible. Apices unornamented around polar raphe endings with single row of areolae on valve mantle. Central area in the form of a rectangular stauros. Striae adjacent to stauros slightly shortened (Fig. 35). Raphe branches straight, of slightly unequal length. Polar raphe endings unilaterally hooked, extending onto valve mantle, towards valve margin, with silica flaps expanding from primary side of valve and accentuating hooked shape of the structure (Fig. 35). Central raphe endings teardrop-shaped, straight.

Internally, raphe slits open centrally onto raised axial rib (Fig. 37). Central raphe endings straight, very slightly expanded. Siliceous knob-like structure between central raphe endings (Fig. 37, arrow). Polar raphe endings straight, simple, completely obscured by well-developed pseudosepta covering ca. 1/6 of valve at each of the apices (Fig. 36). Pseudosepta slightly thickened at open endings. Stauros thickened, especially evident close to valve margin, resembling a reduced butterfly structure typical of *Tursiocola* (Fig. 37).

Up to four girdle bands with single row of perforations (ca. 48 in 10 μm in valvocopula and up to 62 in 10 μm in other copulae).

Supplementary notes.—*Epiphalaina aleutica* was found in six museum specimens of dried whale skin obtained from the Canadian Museum of Nature, Ottawa, Canada. Those samples were collected from the head area of two sperm whales (*Physeter catodon* [*P. macrocephalus*]; samples CANA 126264 and CANA 126273) and four fin whales (*Balaenoptera physalus*; CANA 126260, CANA 126261, CMNMA 57963, and CMNMA 58686) caught in the Canadian Arctic between 1967 and 1972. *E. aleutica* specimens from the sperm whale and fin whale samples did not differ morphologically. They constituted from 94.3% to 100% and from 0.1% to 13.7% of the relative diatom abundance in the sperm whale and fin whale samples, respectively.

Diagnosis.—*Epiphalaina aleutica* differs from *E. radiata*, the only other described species within the genus, in the orientation of the striae at mid-valve, the valve outline, and the width of the pseudosepta as they narrow from the apices (Holmes et al. 1993b). *E. aleutica* has parallel striae at mid-valve while those of *E. radiata* are radiate. *E. radiata* exhibits a slight constriction in the valve outline at mid-valve while the valve outline of *E. aleutica* is not constricted. The pseudosepta of *E. aleutica* rapidly narrow from the apices to very thin strips along the valve margin while the pseudosepta of *E. radiata* narrow to comparatively wider strips.

Plumosigma rimosum T. Nemoto 1956

Figures 38–49

Description.—Valves broadly lanceolate, slightly sigmoid, with rounded apices. Length = 17–26 μm, width = 6.0–8.5 μm, length/width ratio 2.5–3.5; n = 45.

SEM morphology: Externally, valves flat, appearing slightly concave due to weak silicification that may cause them to collapse, bend, or become undulate (Figs. 38–39). Striae (not visible in LM) uniseriate, radiate, slightly arcuate, density = 48–59 in 10 μm, n = 20 (Fig. 38). Areolae roundish to squarish, becoming slightly transapically elongated and rectangular near raphe and strongly transapically elongated towards valve margin, internally occluded by hymenes (Figs. 40, 41, 45). Valve mantle very shallow with smooth margin. Axial area very narrow or missing. Central area small, irregular, asymmetric (Figs. 40, 45). Raphe branches straight; polar raphe endings

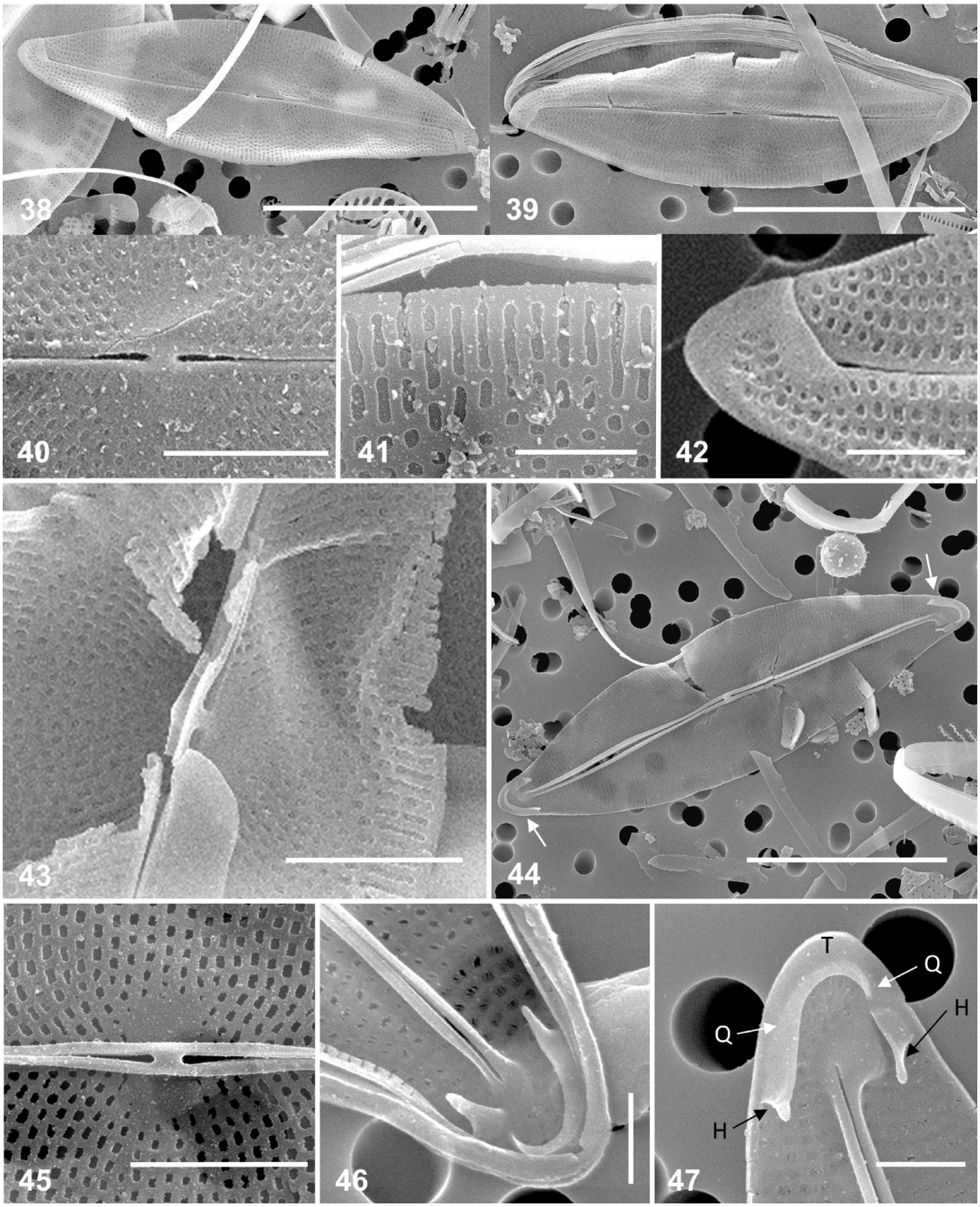

Figs. 38–47: *Plumosigma rimosum*. SEM. Fig. 38, Valve exterior showing lightly silicified valve. Fig. 39, Frustule with partially detached cingulum. Fig. 40, Detail of external central area showing straight, slightly expanded central raphe endings. Fig. 41, Detail of areolae at valve margin exterior. Fig. 42, Detail of exterior deflected polar raphe end fissure. Fig. 43, Oblique view of internal raphe ridge. Fig. 44, Valve interior showing raphe ridge and soleae (arrows). Fig. 45, Detail of internal central area showing straight, slightly expanded central raphe endings. Fig. 46, Detail of solea on valve interior with attached copulae. Fig. 47, Detail of solea showing horseshoe-shape. "H" designates the heels of the solea. "Q" designates the quarters of the solea. "T" designates the toe of the solea. Scale bars: Figs. 38–39, 44 = 10 μm; Figs. 40, 43 = 2 μm; Figs. 41–42, 45–47 = 1 μm.

deflected in opposite directions (Figs. 38–39), reaching valve margin at considerable distance from apices (Fig. 42). Unornamented elongated areas adjacent to polar raphe endings (Fig. 42). Central raphe endings straight, slightly expanded, positioned close to one another (Fig. 40).

Internally, raphe-sternum thickened, raised above flat surface of valve interior (Figs. 44–46). Raphe C-shaped in cross-section creating narrow flange projecting away from raphe (Fig. 43). Internal polar raphe endings with asymmetric helictoglossae whose shape corresponds to that of external polar raphe endings (Figs. 46–47). Central raphe endings straight, slightly expanded, positioned close to one another, separated by small central nodule formed within elevated raphe-sternum (Figs. 44, 45). Shape of areola openings, as well as shape of central area, are same as on the valve exterior. Soleae (described below) at both apices (Figs. 46, 47).

Cingulum with up to four open girdle bands with one row of circular perforations (Fig. 39).

We introduce the term *solea* (plural = *soleae*) to describe the peculiar internal structures, so far only observed in the two currently known *Plumosigma* species – *P. rimosum* and *P. hustedtii* Nemoto 1956. A *solea* (from Latin, "horseshoe") is a horseshoe-shaped siliceous structure that surrounds the helictoglossae, with the heel (H, in Fig. 47) and open end of the horseshoe oriented towards the valve center and the toe (T, in Fig. 47) of the horseshoe at the apex (Fig. 47). The branches, or quarters (Q, in Fig. 47) in horseshoe parlance, of the solea narrow towards the heel and terminate with produced ends. The soleae observed in *P. rimosum* (Figs. 46, 47) are asymmetric, with the asymmetry created by an interruption in the quarter located on the hemivalve on which the external polar raphe ending is deflected. Although the quarters of the soleae of *P. hustedtii* depicted in Plate II, Figs. 5 and 6 in Nagasawa et al. 1990 appear uninterrupted, this impression may be caused by the low resolution of the provided images. The function and morphogenesis of the *solea* are currently unknown.

Supplementary notes.—Plumosigma rimosum was found in four museum specimens of dried whale skin obtained from the Canadian Museum of Nature, Ottawa, Canada. Those samples were collected from the head area of two sperm whales (*Physeter catodon* [*P. macrocephalus*]; samples CMNMA 59235 and CMNMA 59272) and two fin whales (*Balaenoptera physalus*; CANA 126267 and CMNMA 58686) caught in the Canadian Arctic between 1967 and 1972. *P. rimosum* specimens from the sperm whale and fin whale samples did not differ morphologically. They constituted from 0.8% to 1.2% and from 0.5% to 3.2% of the relative diatom abundance in the sperm whale and fin whale samples, respectively. The previously reported anomalous "double valves" (Nagasawa et al. 1990, Pl. 2, Fig. 3) were found in three out of four samples containing *Plumosigma* specimens. The double valves seem to be composed of two valves with a fully developed raphe system and areolae laying directly on each other and connected at the valve margins and possibly the central nodule (Figs. 48–49). The morphogenesis of these anomalous valves remains unknown.

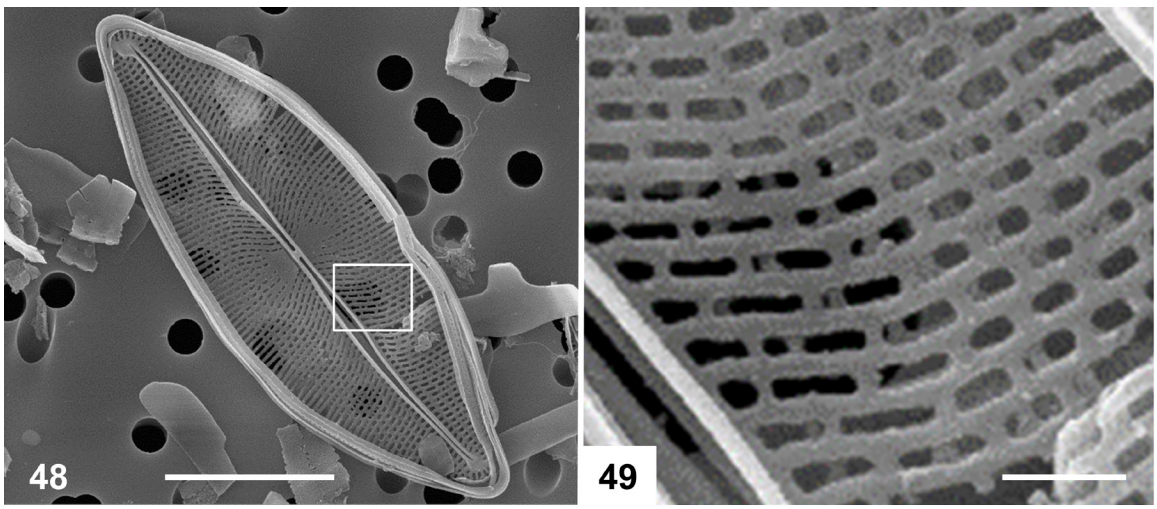

Figs. 48–49: *Plumosigma rimosum*. SEM. Fig. 48, Anomalous double valve interior, rectangle indicates area of detail depicted in Figure 49. Fig. 49, Detail of overlapping areolae of anomalous double valve. Scale bars: Fig. 48 = 5 μm; Fig. 49 = 0.5 μm.

Diagnosis.—*Plumosigma rimosum* differs from *P. hustedtii*, the only other described species within the genus, in the density of the striae and in the areola shape at the valve margin (Nemoto 1956). *P. rimosum* has a greater stria density (48–70 in 10 μm) than *P. hustedtii* (31–55 in 10 μm). The areolae along the valve margin are elongated in *P. rimosum* and round in *P. hustedtii*.

***Bennettella ceticola* (E.W. Nelson) R.W. Holmes 1985**
Figures 50–59

Description.—Frustules heterovalvar with raphid and araphid valves. Valve outline elliptical to rhombic-elliptical. Length = 18–37 μm, width = 11.5–21.5 μm, length/width ratio 1.4–1.8, n = 50.

SEM morphology: Externally, raphid valve face slightly concave with biseriate striae along raphe becoming triseriate and finally tetraseriate on valve mantle (Fig. 50). Tri- and tetraseriate striae are external openings of alveoli that begin at edge of valve face and extend onto valve mantle (Fig. 57). Transapical walls of alveoli evident as ribs along either side of crista marginalis (i.e., marginal ridge that separates valve face from mantle) (Fig. 50, arrow). Crista marginalis wider and more elevated at apices (Fig. 50, arrow). About halfway down valve mantle, tetraseriate openings of alveoli interrupted by narrow band (Fig. 57,

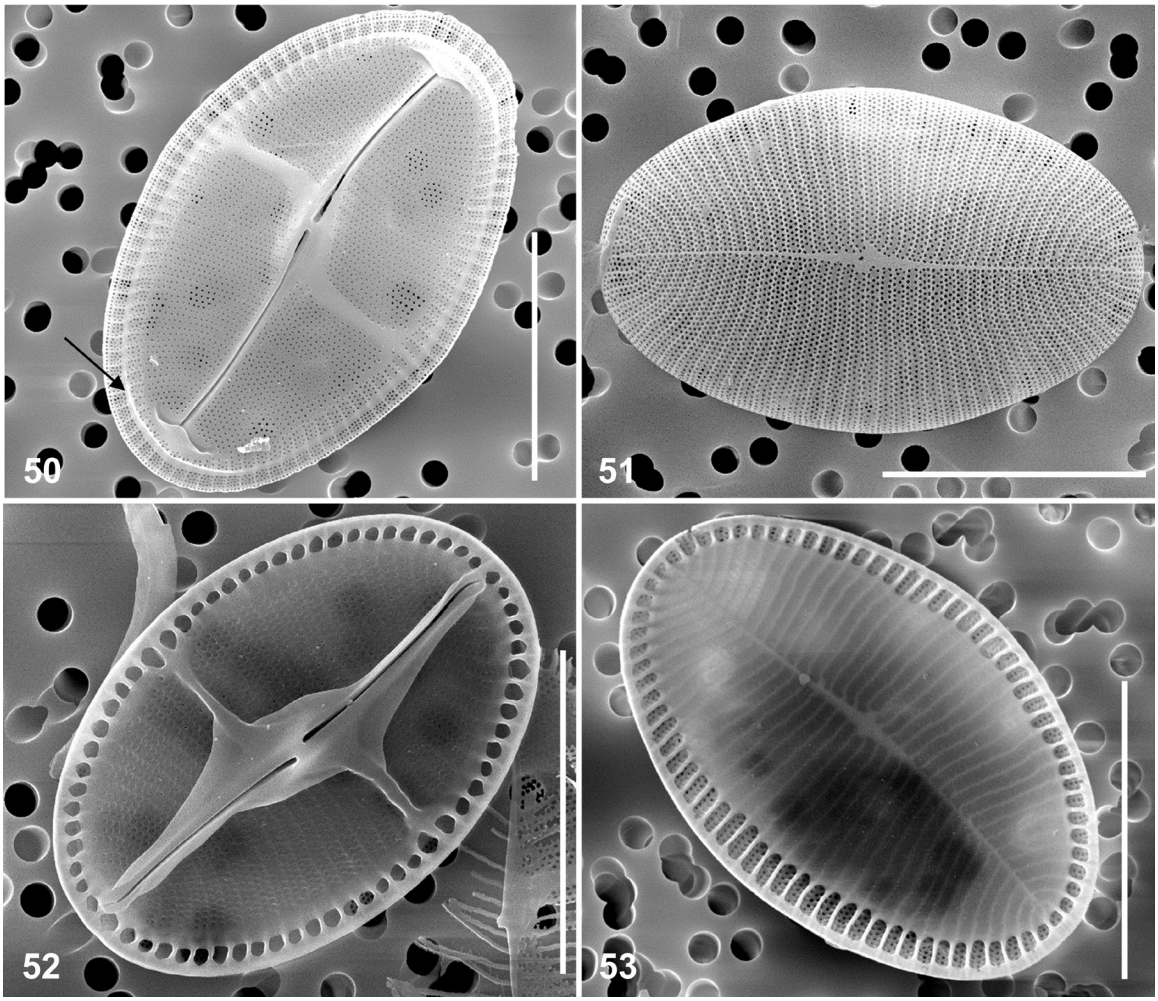

Figs. 50–53: *Bennettella ceticola*. SEM. Fig. 50, Raphid valve exterior showing sigmoid raphe, slightly rhombic-elliptic valve outline, and crista marginalis (arrow). Fig. 51, Araphid valve exterior showing closely spaced triseriate striae and very narrow axial area. Fig. 52, Raphid valve interior showing asymmetric lateral extensions of the raphe-sternum. Note foramina of alveoli along entire valve margin. Fig. 53, Araphid valve interior showing marginal ring of alveolar foramina and unornamented axial plate. Scale bars: Figs. 50–53 = 10 μm.

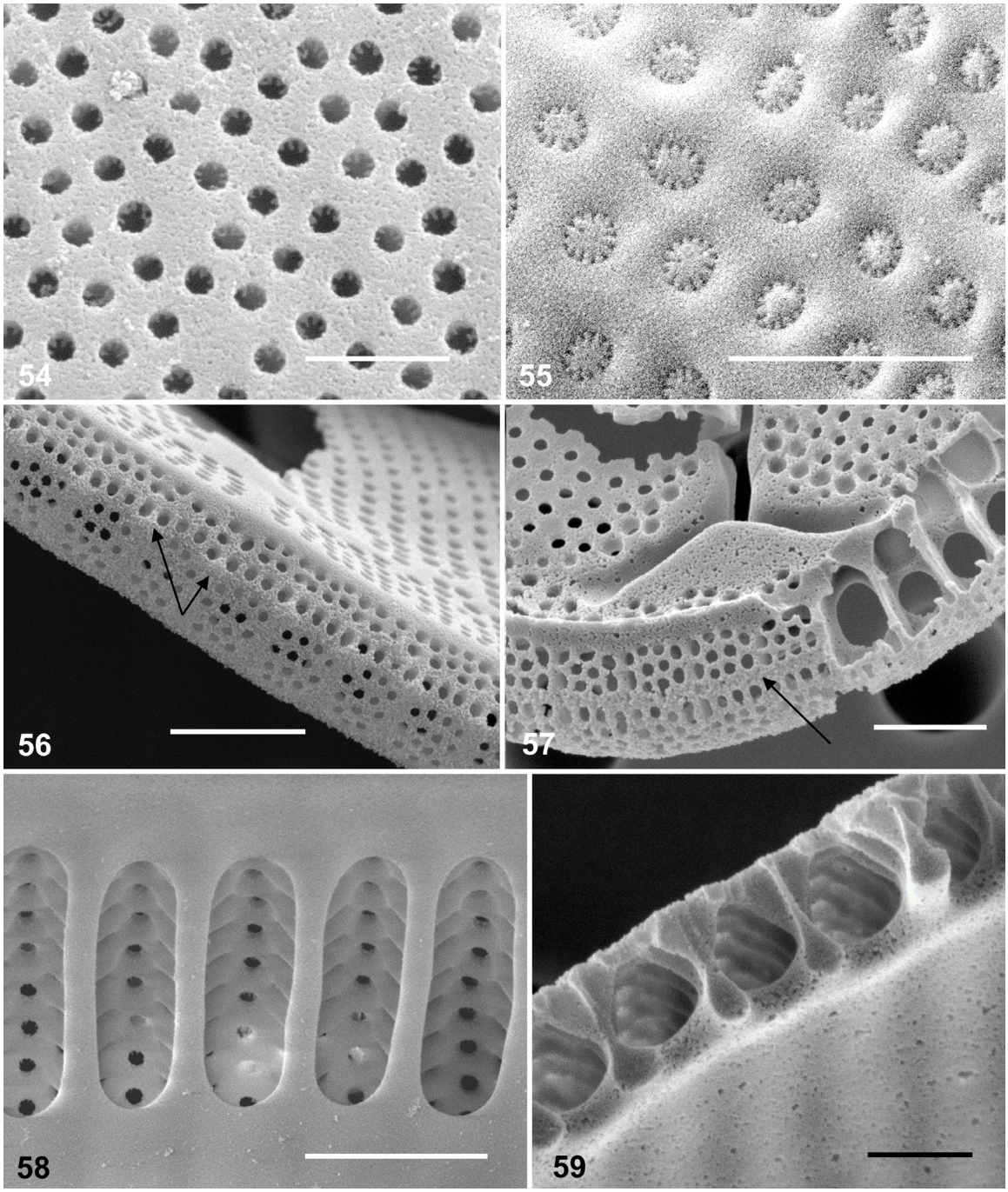

Figs. 54–59: *Bennettella ceticola*. SEM. Fig. 54, Detail of areolae on raphid valve exterior. Fig. 55, Detail of areolae on raphid valve interior. Fig. 56, Detail of raphid valve mantle exterior and nodules on the circumvalvar band (arrows). Fig. 57, Broken raphid valve showing foramina and exterior alveolar openings of marginal alveoli, and circumvalvar band (arrow) on valve exterior. Fig. 58, Detail of araphid valve interior showing marginal foramina and internal view of areolae. Fig. 59, Broken araphid valve depicting internal construction of alveoli and internal valve surface. Scale bars: Figs. 54–55, 59 = 500 nm; Figs. 56–58 = 1 μm.

arrow) ornamented by inconspicuous small nodules (Fig. 56, arrows) where transapical ribs of alveoli intersect with narrow circumvalvar band (Figs. 56–57). Striae nearly straight, parallel to slightly radiate in the valve middle, becoming curved and radiate towards apices, stria density at valve middle = 20–26 in 10 μm, n = 20. Areolae small, round, closely spaced (density 4–5 in 10 μm) (Fig. 54). Axial area very narrow. Raphe sigmoid, with closely positioned, straight, slightly expanded and elongated central raphe endings (Fig. 50). Polar raphe endings obscured by triangular flaps extending from polar portions of valve face, giving the impression of a bifurcated raphe (Figs. 50, 57). The axial area strongly sigmoidal, with lateral extensions narrowing towards valve margin, where it merges with crista marginalis (Fig. 50).

Internally, Raphe-sternum and lateral extensions, similar in shape and position to central and axial areas on the external valve face but wider, thickened and raised above valve face, creating asymmetrical canopy along raphe (Fig. 52). Sigmoid raphe branches lie within middle of raphe-sternum but appear displaced due to asymmetrical shape of canopy. Transapical extensions of the raphe-sternum extend to edge of valve face and expand into flattened unornamented areas (Fig. 52). Oval foramina of marginal alveoli arranged in circumferential ring, 16–18 in 10 μm on valve mantle interior. Central raphe endings elongated, expanded towards thickened and elevated central nodule, slightly deflected in opposite directions (Fig. 52). Internal polar raphe endings deflected in opposite directions and terminate in helictoglossae (Fig. 52). Circular areolae on valve face internally occluded by hymenes with circularly arranged pores along periphery of hymen (Fig. 55).

Externally, araphid valve slightly convex with shallow, steeply sloping mantle (Fig. 51). Double-layered structure of valve evident in cross-section and in eroded specimens (Fig. 59). Central area small, asymmetric, slightly transapically and diagonally expanded, nearly indistinguishable from axial area (Fig. 51). Axial area very narrow, slightly sigmoid, narrowing to a very thin line towards apices (Fig. 51). Striae triseriate (density 17–20 in 10 μm) with small, nearly circular, similarly-sized closely spaced areolae that are somewhat irregularly arranged (density approx. 5–6 in 1 μm) (Fig. 51). Areolae internally occluded by hymenes with circularly arranged pores (Fig. 55). Occasionally, 1–3 irregular, larger or underdeveloped pores within central area.

Internally, araphid valve almost entirely covered by unornamented axial plate with marginal ring of oblong alveolar foramina; density at valve margin = 18–20 in 10 μm.

Copulae open, unornamented. Valvocopula with undulate pars interior.

Supplementary notes.—*Bennettella ceticola* was found in nine museum specimens of dried whale skin obtained from the Canadian Museum of Nature, Ottawa, Canada. The samples were collected from four sperm whales (*Physeter catodon*; CMNMA 59241, CMNMA 59235, CMNMA 59272, CMNMA 59236) and nine fin whales (*Balaenoptera physalus*; CMNMA 58721, CMNMA 58673, CANA 126267, CANA 126260, CANA 126261, CMNMA 58783, CMNMA 58686, CMNMA 57963, CMNMA 57071) caught in the Canadian Arctic between 1967 and 1972. *B. ceticola* specimens from the sperm whale and fin whale samples did not differ morphologically. They constituted from 67% to 100% and from 80.2% to 100% of the relative diatom abundance in the sperm whale and fin whale samples, respectively.

Diagnosis.—*Bennettella ceticola* differs from *B. constricta*, the only other described species within the genus, in the outline of the valve and the in the valve margin of the raphid valve where it meets the stauros (Holmes, 1985). The valve outline of *B. constricta* is constricted while that of *B. ceticola* is not. The valve margin of the raphid valve of *B. constricta* is notched in the valve exterior where the stauros meets the margin, while this feature is lacking in *B. ceticola*.

Epipellis heptunei **Denys and Van Bonn 2001**

Figures 60–65

Description.—Frustules heterovalvar with raphid and araphid valves. Valves broadly oval to nearly circular. Length = 12–17 μm, width = 12–15 μm, n = 22.

SEM morphology: Externally, raphid valve concave with biseriate striae (more evident in internal view) that are curved and radiate around sigmoid raphe-sternum, stria density = 23–29 in 10 μm, n = 11 (Fig. 60). Areolae small, round, closely spaced (density approx. 5 in 1 μm). Striae interrupted on both sides of raphe by unornamented linear areas that extend perpendicularly from raphe-sternum (Fig. 60). These lateral extensions slightly offset from the valve middle and extend to near crista marginalis (Fig. 60,

Figs. 60–65: (page 67) *Epipellis heptunei*. SEM. Figs. 60–63, SEM. Figs. 64–65, LM. Fig. 60, Raphid valve exterior showing sigmoid raphe, lateral extensions of the raphe-sternum, and crista marginalis (arrow). Fig. 61, Raphid valve interior showing biseriate striae, marginal ring of alveoli foramina, and oppositely deflected central raphe endings. Fig. 62, Araphid valve exterior showing very fine striae, an inconspicuous, narrow, sigmoid axial area, and a slightly stepped valve face at the valve face/mantle transition. Fig. 63, Araphid valve interior showing marginal ring of alveolar foramina and shadow lines of alveolate striae. Fig. 64, Live cells brushed from skin surface. Fig. 65, Detail of live cell showing single C-shaped plastid. Scale bars: Figs. 60–65 = 5 μm.

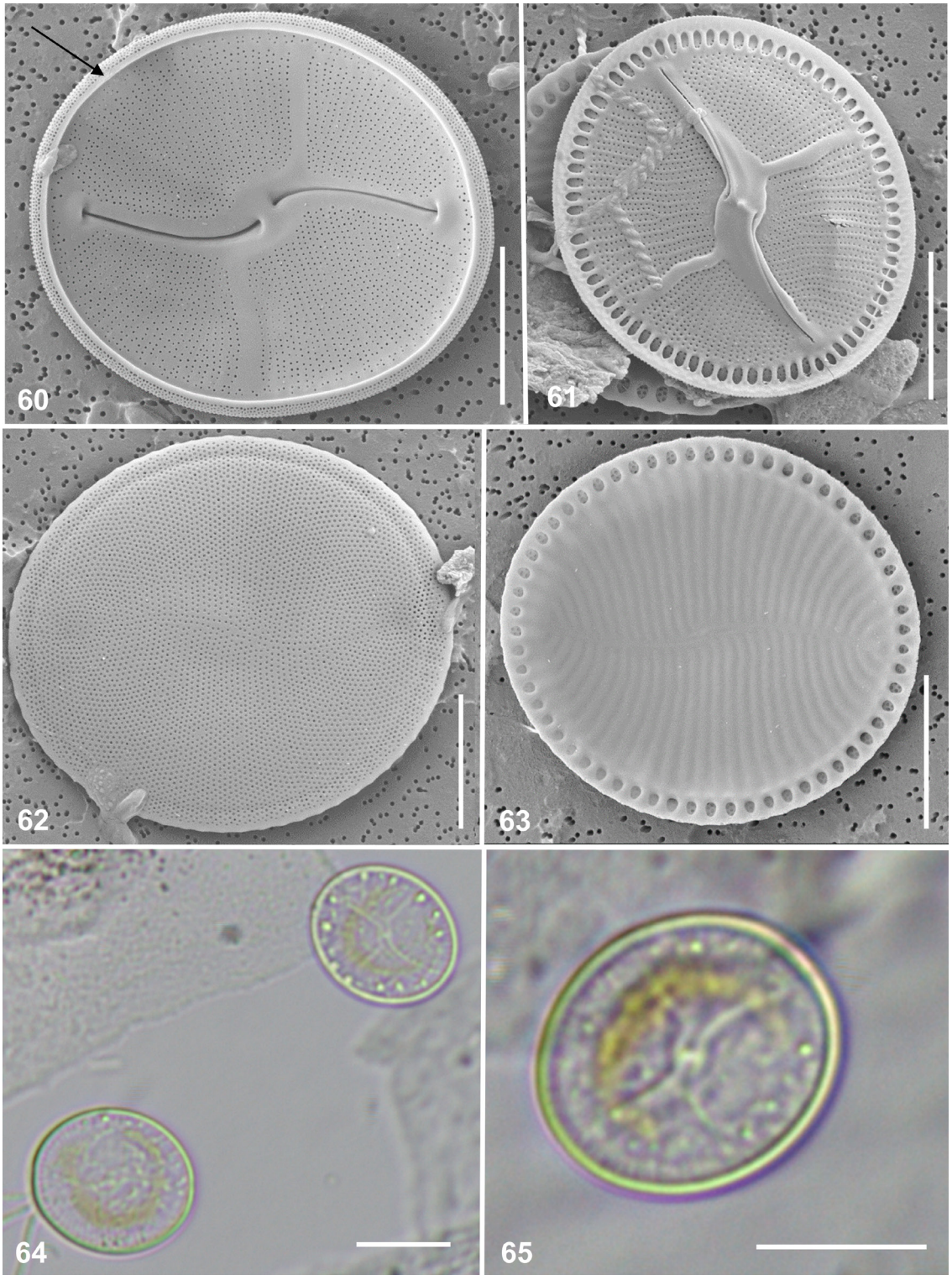

arrow) that arises before valve face/mantle transition area. Outside of crista marginalis, the perimeter of valve face delimited by 3-4 rows of irregularly arranged and very closely spaced (density approx. 9 in 1 um) areolae (Fig. 60). Sigmoid raphe filiform with very slightly expanded central raphe endings. Polar raphe endings terminating a short distance before valve apices in a short transverse depression creating a T-shaped impression.

Internally, raphe-sternum and lateral extensions are thickened and raised above surface of valve interior (Fig. 61). Sigmoid raphe branches lie within middle of raphe-sternum towards apices but become strongly displaced along outside edge of raphe-sternum towards central area. Central raphe endings deflected in opposite directions, slightly expanded, surrounding knob-like structure at center of central nodule (Fig. 61). Internal polar raphe endings straight, simple, lacking helictoglossae. Biseriate character of striae more evident on valve interior as striae are delimited by thickened virgae. Some virgae in middle part of valve bifurcate: however, striae here remain biseriate (Fig. 61). Striae terminating before reaching valve margin where each stria transitions to a marginal alveolus formed from arched struts that connect virgae to unornamented valve margin. Foramina of marginal alveoli elongated ovals, density at valve margin = 18 in 10 μm.

External surface of araphid valve slightly convex, slightly stepped at valve face/mantle transition (Fig. 62). Striae inconspicuously biseriate, curved, radiate around narrow sigmoid sternum, extending to near valve margin, stria density = 23–28 in 10 μm, n = 11. Areolae small, round, closely spaced (density approx. 5 in 1 μm).

Internally, araphid valve nearly covered by unornamented plate with only marginal ring of ovoid foramina, density at valve margin = 15 in 10 μm (Fig. 63). Axial ribs and elongated alveoli that extend from the sigmoid sternum evident as alternating strips of brighter and darker areas on interior valve surface in SEM micrographs. Suggested by differing levels of brightness in SEM micrographs are remnants of infilled raphe in the central area (Fig. 63).

Live cells with large C-shaped plastid lying between valve margin and central area (Figs. 64– 65). Open end of "C" positioned in valve middle.

Supplementary notes.—*Epipellis heptunei* was found in 8 samples from skin areas of 5 individuals of *Tursiops truncatus* during Sarasota Dolphin Research Program health assessments, May 8–12, 2017. *E. heptunei* was observed from all sampled body locations but was most frequent in samples from the axilla ("armpits").

Diagnosis.—*Epipellis heptunei* differs from *E. oiketis*, the only other described species within the genus, in having greater stria and alveolar densities on the raphid valve and greater stria densities on the araphid valve, based on Kliashtorin (1962), Holmes (1985), Denys and Van Bonn (2001), Denys and De Smet (2010), and the present study. Stria densities of *E. heptunei* for the raphid and araphid valves are 22–29 in 10 μm and 22–29 in 10 μm, respectively. The stria densities of *E. oiketis* for the raphid and araphid valves are 10–20 in 10 μm and 12–22 in 10 μm, respectively. The alveolar densities of the raphid valve of *E. heptunei* are 18–22 in 10 μm, while those of *E. oiketis* are 10–16 in 10 μm.

Halamphora baleenicola Stepanek, Frankovich and M.J. Sullivan sp. nov.

Figures 66–79

Description.—LM morphology: Valves semi-elliptical, strongly dorsiventral (Figs. 66–71). Dorsal margin broadly arched. Ventral margin slightly concave. Valve apices rounded, slightly protracted in some specimens. Valve length 43–64 μm, valve width 9–13 μm, n > 351. Raphe weakly arched. Central raphe endings positioned close to each other, dilated, dorsally deflected. Polar raphe endings dorsally deflected. Axial area narrow. Dorsal striae finely areolate, parallel near the valve center, becoming slightly radiate near apices. Stria pattern interrupted at valve middle with appearance of coarser striae and increased areola spacing. Dorsal stria density 28–31 in 10 μm, n = 31. Ventral portion of valve narrow with fine striae difficult to resolve in LM (Figs. 66–71).

SEM morphology: Externally, dorsal stria areolae vary in size, shape, spacing. Areolae small, circular to transapically elongated, oblong (Figs. 72–75). Dorsal areolae irregularly spaced near valve middle (Fig. 73) due to silica infilling of areolae. Ventral striae consisting of 2-3 rows of small areolae, finer and more closely spaced than dorsal striae; stria density 37–43 in 10 μm, n = 15 (Figs. 74–75). Ventral striae more or less interrupted at valve middle with some specimens exhibiting a distinct unornamented area (Fig. 73). Dorsal marginal ridge absent (Fig. 72). Central raphe endings positioned close to each other, slightly deflected, dilated dorsally (Fig. 73). Polar raphe endings slightly deflected dorsally, partially obscured by raphe ledge (Fig. 75). Dorsal raphe ledge continuous, more fully developed near apices and valve center (Figs. 72–74). Ventral raphe ledge absent.

Internally, areolae occluded by hymenes (Fig. 77). Internal raphe-sternum elevated from valve surface on dorsal side (Figs. 76–78). Flange-like structure projecting towards cell interior from the dorsal raphe-sternum at central nodule (Fig. 77). Polar raphe endings as very weakly developed helictoglossae (Fig. 78).

Complete cingula not observed, but separated copulae open, broader dorsally than ventrally, with 2 rows of slit-like areolae separated by unperforated area that is thickened on one side of band (Fig. 79). Copula areolae density 39–45 in 10 μm.

Diagnosis.—Observed in the LM, *Halamphora baleenicola* shares features with several widely distributed marine members of the genus *Amphora*, including *Amphora acuta* W.Gregory, *Amphora arcuata* A.W.F.Schmidt, *Amphora abludens* Simonsen, and *Amphora subhyalina* Podzorski and Håkansson. These taxa all share a similar valve outline, a more or less straight and ventrally appressed raphe, areolate striae, thickened central virgae, and rounded apices. This taxon is distinguished from *A. acuta* by its smaller size and finer striae, with Levkov (2009) reporting valve length of *A. acuta* as 80–140 μm, width as 20–30 μm, and stria density as 14–16 in 10 μm. *A. arcuata* is differentiated by its distinct biarcuate ventral margin and acute apices. Both *A. abludens* and *A. subhyalina* are smaller taxa with finer striae. Stepanek and Kociolek (2018) report valve length as 14–35 μm, width as 4.0–5.5 μm, and stria density as 50–53 in 10 μm for *A. abludens* and valve length as 26–43 μm, width as 5.0–5.5 μm, and stria density as 42–43 in 10 μm for *A. subhyalina* (reported as *A. insulana*, synonym). For *A. subhyalina*, Podzorski and Håkansson (1987) report valve length as 21.3 μm, width as 5.3 μm, and stria density undiscernible in LM and Lobban and Witkowski (2023) report valve length as 27–45 μm, width as 7–8 μm, and stria density as 36–39 in 10 μm. Additionally, *H. baleenicola* lacks the continuous dorsal marginal ridge often visible in all of these *Amphora* species (Levkov, 2009, Stepanek and Kociolek, 2018).

Holotype.—Slide ANSP GC68072 made from the sample ANSP GCM6804 deposited in the Academy of Natural Sciences of Drexel University, Philadelphia, Pennsylvania USA.

Isotypes.—Slides BM 92455 deposited in the Natural History Museum, London, United Kingdom and CANA 131862 deposited in the Canadian Museum of Nature, Ottawa, Ontario, Canada.

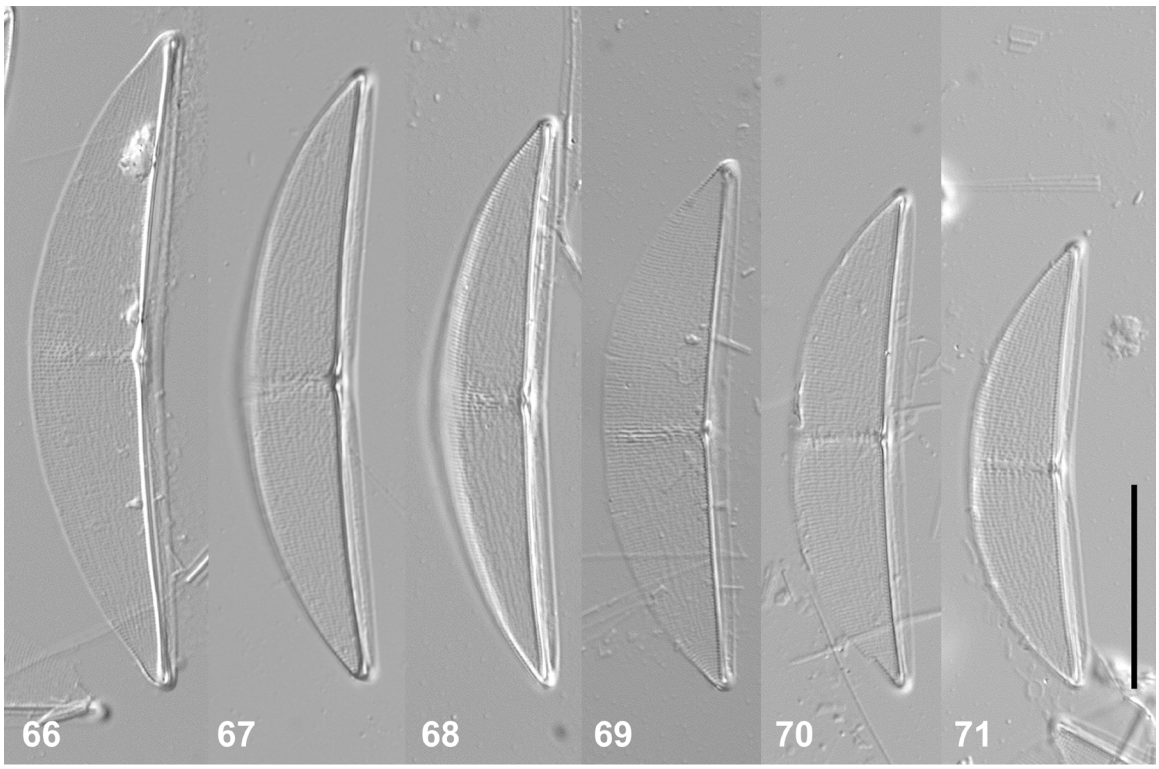

Figs. 66–71: *Halamphora baleenicola* sp. nov. Type population, LM. Valves in valve view showing size range and morphological variation. Scale bar: Figs. 66–71 = 20 µm.

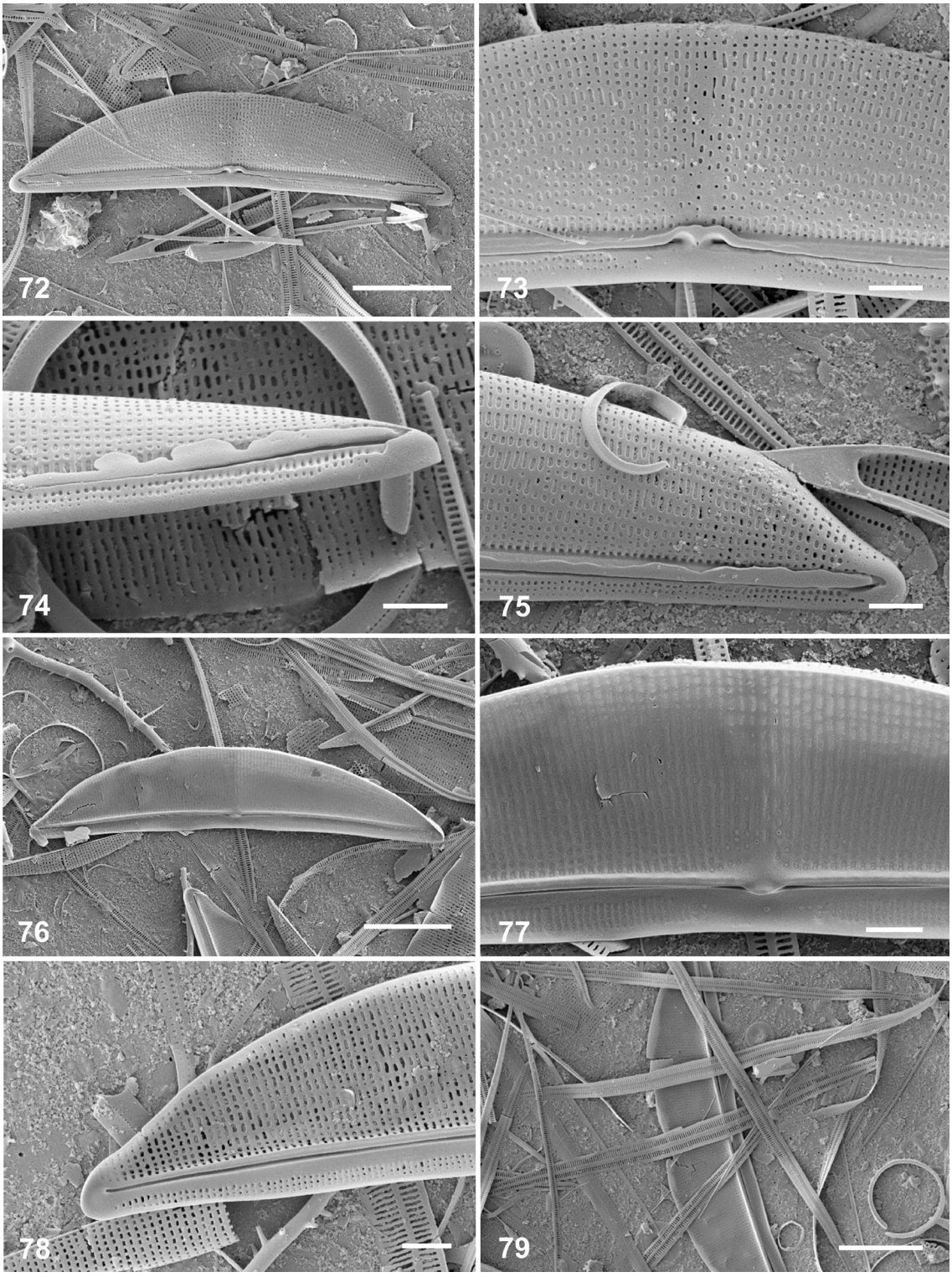

Type locality.—Ocean Shores, Washington USA (46° 56' 29" N, 124° 10' 34" W). Collected from the baleen of a stranded deceased humpback whale *Megaptera novaeangliae* by Jessie Huggins, 27 July 2020.

Etymology.—The epithet *baleenicola* refers to the baleen habitat of the diatom, *-cola* (Latin) = -dweller.

Supplementary notes.—Taxa relative abundances on holotype slide: 9 taxa from 8 genera were observed in a count of 540 valves from the holotype slide ANSP GC68072. The newly described *Halamphora baleenicola* comprised 65% of the valves counted. *Tursiocola cymbelloides* sp. nov. followed in abundance with 25% of the valve count. Planktonic taxa comprised nearly 7% of the assemblage and were represented by *Thalassiosira* spp. and spores of *Chaetoceros radicans* and *Chaetoceros* spp. The remaining 3% of the assemblage consisted of benthic diatoms – *Rhaphoneis amphiceros*, *Anorthoneis* sp., *Tabularia* sp., an undetermined "marine gomphonemoid" and other unidentified taxa, each of which constituted less than 1% of the valve count.

DISCUSSION

This investigation of ceticolous diatoms resulted in the discovery of two new epizoic diatom species from the baleen of humpback and gray whales. The baleen is an often overlooked epizoic habitat with a potentially distinct flora from the skin. Of the 20 previously published studies of ceticolous diatoms listed in Table 1, only Hart (1935) considered baleen as a possible habitat for diatom communities. This habitat was examined in the present study because an orange discoloration was observed on the normally cream-colored baleen of a gray whale (animal number CRC-1740) during the necropsy. The source of the orange discoloration was not ascertained, but in the process *Tursiocola cymbelloides* sp. nov. was found in abundance. This diatom was subsequently found on normally-colored baleen from other gray whales and from the humpback whale stranded on the Washington coast (animal number CRC-1816), which also harbored an abundance of *Halamphora baleenicola* sp. nov. Only incidental (opportunistic) diatoms were observed on the baleen and skin of the one stranded common minke whale examined in Washington and the humpback whale that stranded on the New Jersey coast.

A careful reading of Hart (1935) and his report on the diatoms of the skin film of whales should have prompted subsequent investigations to sample baleen as a likely habitat for ceticolous diatoms. In a short, two-sentence "Note on Baleen Diatoms", Hart (1935) reports on a few scrapings examined from the baleen of "all three species of southern rorquals". As there were four southern rorqual species (blue whale, fin whale, sei whale, and humpback whale) examined, it is uncertain as to which three of the four this refers. Though Hart observed numerous remains of pelagic diatoms on the baleen, he observed three "characteristic species" that "constantly occurred undamaged in large numbers". These three were identified as a *Cymbella* sp. and two *Navicula* spp. The dorsiventral organization of *Cymbella* spp. suggests that the "*Cymbella"* he observed but did not illustrate could be *Halamphora baleenicola* sp. nov., or the new "cymbelloid" *Tursiocola cymbelloides* sp. nov. The two *Navicula* spp. could be *Tursiocola* spp. Hart's drawing of a *Navicula* sp. from the skin of a sperm whale (Hart 1935 Plate XI, Fig. 8) depicts cells with opaque areas at the apices and across the cell middle that may correspond to the characteristic pseudosepta and butterfly structure, respectively, of the *Tursiocola* genus. *Halamphora baleenicola* sp. nov. and *Tursiocola cymbelloides* sp. nov. may be re-discoveries of two of Hart's baleen diatoms. Conversely, *H. baleenicola* sp. nov. may have occurred incidentally. The present observation is limited to just one animal and the number of observations from baleen samples are still very small. It is also likely that multiple pennate diatom species are adapted to this unusual habitat provided only by baleen whales. Thus, it should be expected that new sampling efforts will result in new diatom species discoveries.

Tursiocola cymbelloides sp. nov. adds a 15th species to this still exclusively epizoic diatom genus and expands the known number of cetacean species that serve as hosts for its members. The new species is notable within the genus because of the strongly dorsiventral organization of the

Figs. 72–79: (page 70) *Halamphora baleenicola* sp. nov. Type population, SEM. Fig. 72, Valve exterior showing broadly arched valve outline and impression of interrupted dorsal striae at valve middle. Fig. 73, Detail of external central area showing closely spaced central raphe endings and infilling of the dorsal poroid areolae at valve middle. Fig. 74, Detail of valve apex. Note dorsal raphe ledge and partially developed conopeum. Fig. 75, Detail of external dorsal and ventral striae at valve apex. Note dorsal raphe ledge and partially developed conopeum and interior valve view of *Tursiocola cymbelloides* on right. Fig. 76, Valve interior showing the internal raphe-sternum elevated from the valve surface on the dorsal side. Fig. 77, Detail of internal central area showing central flange that projects from the dorsal raphe-sternum and obscures the internal central raphe endings. Fig. 78, Detail of internal valve apex showing weakly developed helictoglossa. Fig. 79, Unattached copulae with 2 rows of slit-like areolae separated by an unperforated area that is thickened on one side of the band. Scale bars: Figs. 72, 76, 79 = 10 μm, Figs. 73–75, 77–78 = 2 μm.

frustule. Live cells were not observed of *T. cymbelloides* sp. nov. nor of *Halamphora baleenicola* sp. nov., so the mode of nutrition is unknown for both species. Interestingly, Hart (1935) described "colourless cell contents" of the three characteristic baleen diatoms he observed, suggesting that these diatoms might be heterotrophic, as are some *Tursiocola* species on manatees (Frankovich et al., 2018; Majewska and Goosen, 2020).

Halamphora baleenicola sp. nov. is currently the only representative of *Halamphora* to be abundant as a ceticolous diatom, though the genera *Amphora* Ehrenberg ex Kützing 1844 and *Halamphora* (Cleve 1895) Levkov 2009 are well represented in benthic marine communities. *H. baleenicola* shares several morphological features with members of the *Amphora* clade A group (sensu Stepanek and Kociolek, 2019), specifically the species *A. acuta*, *A. abludens*, and *A. subhyalina* that would have been historically classified within Cleve's (1895) subgenus *Oxyamphora*. These taxa share a highly dorsiventral, semi-elliptical to semi-lanceolate valve shape, a more or less straight ventral margin and raphe, rounded valve poles, fine and somewhat irregularly areolate striae, and more or less thickened central virgae (Levkov, 2009; Stepanek and Kociolek, 2018, 2019). Although superficially similar, Stepanek and Kociolek (2019) and Stepanek et al. (2023) have discussed the plesiomorphic nature of many of the putative features used to distinguish *Amphora* clade A and *Halamphora* taxa and the systematic difficulties this can cause. This taxon, once again, highlights this challenge as it exhibits plesiomorphic features shared by both genera.

In the SEM, *Halamphora baleenicola* exhibits a flange-like structure projecting towards the cell interior from the dorsal raphe-sternum at the central nodule (Fig. 77), a marked difference between dorsal and ventral striae densities (Fig. 75), dilated and dorsally deflected central raphe endings (Fig. 73), lack of a dorsal marginal ridge (Fig. 72), and copula ornamented with two rows of elongate areolae (Fig. 79). While these features are not individually diagnostic of *Halamphora* to the exclusion of *Amphora*, they are nonetheless all far more common within *Halamphora*, with a thickened projection on the internal central nodule, striae differentiation, lack of a dorsal marginal ridge, and copula ornamentation not seen in any other *Amphora* clade A species (Stepanek and Kociolek, 2018, 2019). Taken together, these features support the placement of this taxon within *Halamphora*.

Examination of ceticolous diatoms on the museum skin specimens revealed morphologies not previously described and expanded our knowledge of the distribution of epizoic diatoms across different host species and geographical locations. The observation of *Tursiocola staurolineata* on a museum skin specimen from a sperm whale is the first recording of this diatom species since its original description, though Denys (1997) also recognized this diatom in specimens illustrated in Holmes et al. (1993a) which they mistakenly identified as *Tursiocola olympica* from Dall's porpoises. The known distribution of *T. staurolineata* is on sperm whales (2 observations) and Dall's porpoises (within multiple colonies on multiple individuals) from the North Atlantic, North Pacific, and Arctic oceans.

Samples from the museum preparation also allowed us the opportunity to study the frustule of some known ceticolous diatoms in greater detail. For example, examination of *Epiphalaina aleutica* using scanning electron microscopy of greater resolution than that used by Holmes et al. (1993a) and Denys (1997) revealed the presence of a rudimentary butterfly structure (Fig. 37). The butterfly structure is a non-perforate silica membrane on the valve interior that projects from extensions of the pseudosepta at the valve middle to the central area adjacent to the raphe ledge. The membrane forms roofed chambers on each side of the raphe ledge that are open towards the apices (Holmes et al.,1993a, and figs. 42, 77, 100 in Frankovich et al., 2018). Majewska (2020) further described the butterfly structure as a "variably developed stauros-like structure, which should not be interpreted as a true stauros, appearing as the transverse thickening in the valve middle, not reaching the central nodule and merging with the valve margins". The structure was named the "butterfly-like" structure by Denys (1997). The presence or absence of the butterfly structure served as the primary distinction between *Tursiocola* and *Epiphalaina* (Holmes et al., 1993a; Denys, 1997). The higher resolution observations of the internal central area of *E. aleutica* in the present study revealed that thickened silica membranes project from the middle valve margins and connect to the valve face interior without forming chambers (Fig. 37). The rudimentary butterfly structure of *E. aleutica* projects from very narrow and nearly inconspicuous extensions of the pseudosepta (Fig. 37, black arrowheads). The existence of a rudimentary butterfly structure blurs the distinction between *Tursiocola* and *Epiphalaina*. Differently arranged hymen pores were presented as another distinction between *Epiphalaina* and *Tursiocola* by Holmes et al. (1993a), but Majewska and Goosen (2020) discussed observations of varying hymen pore arrangements within *Tursiocola ziemanii* Frankovich and M.J.Sullivan casting further doubt about distinctions between the two genera. The new observations of the rudimentary butterfly structure in *Epiphalaina aleutica* further supports the hypothesis that *Tursiocola* is paraphyletic as indicated by a cladistic analysis of morphological characters that suggested *Epiphalaina*

species were derived taxa within the *Tursiocola* clade (Frankovich et al., 2018). Keeping these two genera as separate entities is becoming increasingly tenuous.

The valve length, width, length to width ratio and stria densities of the *Epiphalaina* specimens of the present study are within the ranges produced for both *E. aleutica* var. *aleutica* and *E. aleutica* var. *lineata* Denys (see Table 1 in Denys, 1997). The slightly narrower valves of *E. aleutica* var. *lineata* (1.9–3 μm) versus those of *E. aleutica* var. *aleutica* (2.7–4.1 μm) were used to propose the distinct variety (Denys, 1997), but the overlap of the valve width of the present specimens (2.2–3.0 μm) with both varieties weakens the argument for separate varieties.

The known distribution of *E. aleutica* is on sperm whales (2 observations), Dall's porpoises (multiple individuals), and also on fin whales from the North Atlantic, North Pacific, and Arctic oceans.

SEM observations of *Plumosigma rimosum* provided ultrastructural details of the newly named "soleae", peculiar internal structures associated with the polar raphe endings. Nagasawa et al. (1990) first described these as a "thickened U-shaped helictoglossa" or anchor-like structures in *P. hustedtii*. The location of the soleae and their possible connection with the helictoglossae (Plate II, Fig. 6 in Nagasawa et al., 1990) and apical portion of the valve (Figs. 46, 47) may suggest that soleae are merely modified helictoglossae or pseudosepta, but the separation of the solea from the valve margin (Figs. 44, left apex; Plate II, Fig. 6 in Nagasawa et al., 1990) and from the helictoglossae (Figs. 44, 46, 47) in other specimens argue for a separate structure. The ultrastructural differences of the soleae depicted in *P. hustedtii* (Nagasawa et al., 1990) and those of *P. rimosum* in the present study may provide an additional species-level diagnostic character, but additional material should be examined before making this conclusion.

Nemoto (1956) described two species of *Plumosigma* (*P. hustedtii* and *P. rimosum*) from multiple, unspecified host whale species. Though he did not provide a direct diagnosis, it is evident from slight differences in the species descriptions that the species were differentiated based on differences in stria density and valve apex shape. *P. hustedtii* was described as having rounded apices and a stria density of 35–45 in 10 μm while *P. rimosum* was described as having acute apices and a stria density of 50–70 in 10 μm. The shape of the valve apices in the six illustrations of valves of both species (Nemoto, 1956) all appear similarly rounded and do not support an argument for differences in valve shape. Nagasawa et al. (1990) further described *P. hustedtii* and *P. rimosum* from sperm whales captured in the North Pacific Ocean. They identified and differentiated the species in accordance with the reported stria density differences of Nemoto (1956). They report stria densities of 31–40 in 10 μm at valve center and 40–55 in 10 μm at the apices for *P. hustedtii*, but did not produce measurements for *P. rimosum* because of the stated scarcity of that species. They also described differences in areola shape between the two species with *P. hustedtii* having round areolae while *P. rimosum* having elongated areolae along the valve margin. The *Plumosigma* specimens of the present study exhibited stria densities of 48–59 in 10 μm and elongated areolae along the valve margin (Figs. 38, 39, 41, 43); both observations are consistent with the original description of *P. rimosum* and later observations by Nagasawa et al. (1990). The known distribution of *Plumosigma* species is on sperm whales, Dall's porpoises (1 specimen reported in Nagasawa et al., 1990), and now also fin whales from the North Atlantic, North Pacific, and the Arctic.

Bennettella ceticola is the most commonly reported ceticolous diatom, having been observed on the greatest number of different cetacean host species and individuals (Bennett, 1920; Hart, 1935; Nemoto, 1958; Holmes, 1985; Gerasimiuk and Zinchenko, 2012; Ferrario et al. 2019). SEM observations of the present study provided the first description of the hymenate pore occlusions on the interior of the raphid valve of *B. ceticola*. The circular arrangement of perforations on the periphery of the hymen (Fig. 55) are similar to those of *Cocconeis* sp. 9 in Riaux-Gobin and Romero (2003, Plate 52, Figure 5) providing possible further evidence for a close relationship with that genus. Ferrario et al. (2019) emended the original description of *Bennettella* R.W.Holmes 1985 by providing the first ultrastructural description of the external polar raphe endings. They revealed that the raphe ends are not bifurcated but are obscured by a triangular flange (Figs. 50, 57), placing *Bennettella* in closer relation to the similarly alveolate genus *Epipellis*. Ferrario et al. (2019) also illustrated the complex ribbed margin of the external mantle of the raphid valve. A more detailed view of the valve mantle (Fig. 56, arrows), however, reveals a small nodule on each of those ribs. The internal construction of the alveoli of the araphid valve is also illustrated for the first time here revealing arched internal ceilings of the alveoli (Figs. 58, 59). Observations of *B. ceticola* on stranded harbor porpoises in Puget Sound, Washington, USA expand the known distribution of the diatom species to 12 host cetacean species. The other host species are northern right whale, blue whale, fin whale, sei whale, gray whale, humpback whale, minke whale, southern minke whale, sperm whale, Dall's porpoise, La Plata dolphin, and Cuvier's beaked whale.

This study's observations of *Epipellis oiketis* on harbor porpoises in Puget Sound Washington, USA and *Epipellis heptunei* on bottlenose dolphins in Sarasota Bay,

Florida, USA are consistent with the previously published distributions of the two diatom species. *E. oiketis* was described by Holmes (1985) based on specimens from Dall's porpoises in the North Pacific but the taxon to which the name is applied includes the invalidly published, but earlier described, *Cocconeis orcii* Kliashtorin 1962 collected from a North Pacific killer whale. *E. oiketis* has also been observed on a sperm whale and unspecified baleen whales in the colder waters of the North Pacific as summarized in Denys (1997). *E. heptunei* has not been recorded since the original description prior to this study. The present study's observation of a single C-shaped plastid in live specimens further suggests a close relationship with *Bennettella* (Ferrario et al., 2019) and *Cocconeis* (Round et al., 1990; Cox, 1996). *E. heptunei* has been observed only on bottlenose dolphins residing in latitudes lower than the known geographic range of *E. oiketis*.

Denys and De Smet (2010) distinguished *E. heptunei* from *E. oiketis* based on four differences in valve morphology. They described greater stria and alveolar foramina densities in *E. heptunei*, as well as 3–4 rows of poroids on the slope of the crista marginalis of *E. heptunei* versus 2 rows in *E. oiketis*. They also described a C-shaped raised embossment around the polar raphe endings on the interior of the RV valve that is present on *E. heptunei* but lacking in *E. oiketis* specimens they studied. The SEM observations of the crista marginalis in *E. heptunei* of the present study (Fig. 58) are consistent with the original description, but the distinction of a C-shaped embossment at the RV internal polar raphe endings was not evident in the Florida specimens from bottlenose dolphins. The determination of *E. oiketis* on the stranded harbor porpoises from Puget Sound was based on LM examination only and measured stria densities on the araphid valves (i.e., 13 in 10 μm) that were consistent with the species description and diagnosis.

This study described two new ceticolous diatoms that may be rediscoveries of diatoms briefly mentioned by Hart (1935). Baleen has been re-confirmed as a novel habitat for diatoms. This study also added four additional cetacean species to the still relatively short list of cetaceans that have been examined microscopically and taxonomically for ceticolous diatoms. Though the four cetacean species did not provide sufficient numbers of epizoic diatoms for detailed study, these negative results do not preclude the possibility of finding ceticolous diatoms on these species in future examinations. As demonstrated in this study, continued examination of ceticolous diatoms will provide new knowledge concerning their distributions, morphological characterizations, and insights into the origin and evolution of these unique epizoic diatom communities.

ACKNOWLEDGMENTS

We are grateful to the staff, students, volunteers, and the scientific and veterinary collaborators of the Sarasota Dolphin Research Program for making bottlenose dolphin sample collection possible. Primary funding for the health assessment project was provided by Dolphin Quest, Inc. We thank The Whale Museum, Friday Harbor, Washington for their assistance with the minke whale stranding, and Washington Department of Fish and Wildlife Marine Mammal investigations for assistance with a gray whale and a harbor porpoise stranding. We thank Bob Schoelkopf, Marine Mammal Stranding Center, Brigantine, New Jersey for assistance with a humpback whale stranding. We thank Art Cooper and Jillian Schwartz, Dolphins Plus Marine Mammal Responder, Key Largo, Florida for assistance with *Kogia* sp. and Gervais's beaked whale strandings. We thank Stéphanie Tessier, Canadian Museum of Nature, Ottawa, Canada, for her invaluable support and infinite enthusiasm during the diatom extraction from the museum specimens of the whale skin and Michel Poulin, Canadian Museum of Nature, Ottawa, Canada, for his support during the research visit to the museum. We are further grateful to William E. Goosen, Jan Neethling, and other staff from the Centre for High Resolution Transmission Electron Microscopy, Nelson Mandela University, Gqeberha, South Africa, for their generous help during the SEM analyses. This work received partial financial support from the Canadian Museum of Nature, Ottawa, Canada, through the Visiting Scientist Award granted to R. Majewska (2018). We also thank Nicole Stacy, University of Florida for assistance with permits. This material is based upon work supported by the National Science Foundation under Grant No. 2331644. This is contribution number 2022 from the Institute of Environment at Florida International University.

LITERATURE CITED

Anonymous. 1975. Proposals for a standardization of diatom terminology and diagnoses. Beihefte zur Nova Hedwigia 53: 323–354.

Ashworth, M.P., R. Majewska, T.A. Frankovich, M. Sullivan, S. Bosak, K. Filek, and S.R. Manning. 2022. Cultivating epizoic diatoms provides insights into the evolution and ecology of both epibionts and hosts. Scientific Reports 12: 15116.

Azari, M., Y. Farjad, A. Nasrolahi, M. De Stefano, M. Ehsanpour, S. Dobrestov, and R. Majewska.2020. Diatoms on sea turtles and floating debris in the Persian Gulf (Western Asia). Phycologia 59: 292–304.

Bennett, A.G. 1920. On the occurrence of diatoms on the skin of whales. Proceedings of the Royal Society of London Series B 91: 352–357.

Cleve, P.T. 1895. Synopsis of naviculoid diatoms. II. Kongliga Svenska Vetenskaps Akademiens Handlingar, 27, p. 219.

Cox, E.J. 1996. Identification of freshwater diatoms from live material. Chapman and Hall, New York, p. 160.

Cox, E.J. 2012. Ontogeny, homology, and terminology – Wall morphogenesis as an aid to character recognition and character state definition for pennate diatom systematics. Journal of Phycology 48: 1–31.

Denys, L. 1997. Morphology and taxonomy of epizoic diatoms (*Epiphalaina* and *Tursiocola*) on a sperm whale (*Physeter macrocephalus*) stranded on the coast of Belgium. Diatom Research 12: 1–18.

Denys, L., and W.H. De Smet. 2010. *Epipellis oiketis* (Bacillariophyta) on harbor porpoises from the North Sea Channel (Belgium). Polish Botanical Journal 55: 175–182.

Denys, L., and W. Van Bonn. 2001. A second species in the epizoic diatom genus *Epipellis*: *E. heptunei* sp. nov., p. 167–176 *In*: R. Jahn, J.P. Kociolek, A. Witkowski, and P. Compère (eds.). Lange-Bertalot Festschrift. Studies on diatoms. Dedicated to Prof. Dr. Horst Lange-Bertalot on the occasion of his 65th birthday, A.R.G. Gantner Verlag, Ruggell, Liechtenstein.

Ferrario, M. E., A.O. Cefarelli, A. Fazio, P. Bordino, and O.E. Romero. 2019. *Bennettella ceticola* (Nelson ex Bennett) Holmes on the skin of Franciscana dolphin (*Pontoporia blainvillei*) of the Argentinean Sea: an emendation of the generic description. Diatom Research 33: 485–497.

Frankovich, T.A., M.P. Ashworth, M.J. Sullivan, J. Veselá, and N.I. Stacy. *Medlinella amphoroidea* gen. et sp. nov. (Bacillariophyta) from the neck skin of Loggerhead sea turtles (*Caretta caretta*). Phytotaxa 272: 101–114.

Frankovich, T.A., M.J. Sullivan, and N.I. Stacy. 2015. Three new species of *Tursiocola* (Bacillariophyta) from the skin of the West Indian manatee (*Trichechus manatus*). Phytotaxa 204: 33–48.

Frankovich, T.A., M.P. Ashworth, M.J. Sullivan, E.C. Theriot, and N.I. Stacy. 2018. Epizoic and apochlorotic *Tursiocola* species (Bacillariophyta) from the skin of Florida manatees (*Trichechus manatus latirostris*). Protist 169: 539–568.

Gerasimiuk, V.P., and V.L. Zinchenko. 2012. Diatom fouling of the little piked whales in the Antarctic waters. Hydrobiological Journal 48: 28–34. [In Russian.]

Goldin, E.B. 2010. Epibiont algal flora of bottlenose dolphins in Black Sea dolphinariums. Ecosystems, their optimization and protection 2: 21–29. [In Russian.]

Hart, T.J. 1935. On the diatoms of the skin film of whales and their possible bearing on problems of whale movements. Discovery Reports 10: 247–282.

Hasle, G.R., and E.E. Syvertsen. 1997. Marine diatoms, p. 5–385 *In*: Tomas, C.R. (ed.). Identifying marine phytoplankton. Academic Press, San Diego.

Holmes, R.W. 1985. The morphology of diatoms epizoic on cetaceans and their transfer from *Cocconeis* to two new genera, *Bennettella* and *Epipellis*. British Phycological Journal 20: 43–57.

Holmes, R.W., and S. Nagasawa. 1995. *Bennettella constricta* (Nemoto) Holmes and *Bennettella berardii* sp. nov. (Bacillariophyceae: Chrysophyta) as observed on the skin of several cetacean species. Bulletin of the National Science Museum, Tokyo Series B 21: 29–43.

Holmes, R.W., S. Nagasawa, and T. Nemoto. 1989. Epidermal diatoms on the Dall's porpoise landed at Otsuchi, Iwate, Japan. Otsuchi Marine Research Center Reports 15: 15–20.

Holmes, R.W., S. Nagasawa, and H. Takano. 1993a. The morphology and geographic distribution of epidermal diatoms of the Dall's porpoise (*Phocoenoides dalli* True) in the Northern Pacific Ocean. Bulletin of the National Science Museum, Tokyo Series B 19: 1–18.

Holmes, R.W., S. Nagasawa, and H. Takano. 1993b. A re-examination of diatom samples obtained from cetaceans collected off South Africa. Bulletin of the National Science Museum, Tokyo Series B 19: 127–135.

Hustedt, F. 1952. Diatomeen aus der Lebengemeinschaft des Buckelwals (*Megaptera nodosa* Bonn.). Archiv für Hydrobiologie 46: 286–298.

Kawamura, A. 1992. Notes on the pattern of diatom fouling in three southern rorqual species. Bulletin of the Faculty of Bioresources, Mie University 8: 19–26.

King 5 Staff. 2019. Emaciated gray whale found dead in southern Puget Sound inlet. https://www.king5.com/article/news/dead-gray-whale-found-in-puget-sound-inlet/281-27e84a03-b517-4609-8b5e-da1496846d3f#:~:text=The%20whale%20was%20found%20in%20Budd%20Inlet%2C,Research%20said%20the%20whale%20was%20%22very%20emaciated.%22

King 5 Staff. 2020. Beached whale in Ocean Shores died from 'blunt force trauma'. https://www.king5.com/article/tech/science/environment/beached-whale-ocean-shores-died-blunt-force-trauma/281-677be15e-4eb1-426d-b77f-63a7d9b35ba6

Kliashtorin, L.B. 1962. The diatoms of the skin film of whales in the Far-Eastern Seas. Trudy Instituta Okeanologii, Akademija Nauk USSR 58: 314–321. [In Russian.]

Levkov, Z. 2009. *Amphora* sensu lato. *In*: H. Lange-Bertalot (ed.), Diatoms of Europe, Volume 5. Ruggell, A.R.G. Gantner Verlag K.G., Liechtenstein.

Lobban, C.S., and A. Witkowski. 2023. Marine benthic diatoms of Guam: new records, *Dictyoneis apapae* sp. nov., and updates to the checklist. Micronesica 2023: 1–75.

Majewska, R. 2020. *Tursiocola neliana* sp. nov. (Bacillariophyceae) epizoic on South African leatherback sea turtles (*Dermochelys coriacea*) and new observations on the genus *Tursiocola*. Phytotaxa 453: 1–15.

Majewska, R., M.P. Ashworth, S. Bosak, W.E. Goosen, C. Nolte, K. Filek, B. Van de Vijver, J.C. Taylor, S.R. Manning, and R. Nel. 2020. On sea turtle-associated Craspedostauros (Bacillariophyta), with description of three novel species. Journal of Phycology 57: 199–218.

Majewska, R., M.P. Ashworth, E. Lazo-Wasem, N.J. Robinson, L. Rojas, et al. 2018. *Craspedostauros alatus* sp. nov., a new diatom (Bacillariophyta) species found on museum sea turtle specimens. Diatom Research 33: 229–240.

Majewska, R., and W.E. Goosen. 2020. For better, for worse: manatee□associated *Tursiocola* (Bacillariophyta) remain faithful to their host. Journal of Phycology 56: 1019–1027.

Majewska, R., B. Van de Vijver, A. Nasrolahi, M. Ehsanpour, M. Afkhami, F. Bolaños, and M. De Stefano. 2017. Shared epizoic taxa and differences in diatom community structure between green turtles (*Chelonia mydas*) from distant habitats. Microbial Ecology 74*:*, 969–978.

Morejohn, G.V. 1980. The Natural History of Dall's Porpoise in the North Pacific Ocean, p. 45–84 *In*: H.E. Winn, and B.L. Olla (eds.), Behavior of Marine Animals, Current Perspectives in Research, Volume 3: Cetaceans). Plenum Press, New York.

Nagasawa, S., R.W. Holmes, and T. Nemoto. 1990. The morphology of the cetacean diatom genus *Plumosigma* Nemoto. Scientific Reports of Cetacean Research 1*:* 85–91.

Nemoto, T. 1956. On the diatoms of the skin film of the whales in the Northern Pacific. The Scientific Reports of the Whales Research Institute, Tokyo 11: 99–132.

Nemoto, T. 1958. *Cocconeis* diatoms infected on whales in the Antarctic. The Scientific Reports of the Whales Research Institute, Tokyo 13: 185–192.

Nemoto, T., R.L. Brownell Jr., and T. Ishimaru. 1977. *Cocconeis* diatom on the skin of Franciscana. The Scientific Reports of the Whales Research Institute, Tokyo 29: 101–105.

Nemoto, T., P.B. Best, K. Ishimaru, and H. Takano. 1980. Diatom films on whales in South African waters. The Scientific Reports of the Whales Research Institute, Tokyo 32: 97–103.

Okuno, H. 1954. Electron-microscopical study on Antarctic diatoms. The Journal of Japanese Botany 29: 15–22.

Omura, H. 1950. Diatom Infection on Blue and Fin whales in the Antarctic Whaling Area V (the Ross Sea Area). The Scientific Reports of the Whales Research Institute, Tokyo 4: 14–26.

Podzorski, A.C., and H. Håkansson. 1987. Freshwater and marine diatoms from Palawan (a Philippine island). Bibliotheca Diatomologica, Band 13. J. Cramer, Berlin, p. 245.

Proschkina-Lavrenko, A.I. 1961. Diatomeae novae e Mari Nigro (Ponyo Euxino) et Azoviano (Maeotico). Notulae Systematicae e Sectione Cryptogamica Instituti Botanici nomine V.L. Komarovii Academiae Scientiarum USSR 14: 33–39. [In Russian.]

Reicher, M. 2020. https://www.seattletimes.com/seattle-news/environment/gray-whale-washes-ashore-on-bainbridge-island-fifth-on-west-coast-this-year/

Riaux-Gobin, C., and O. Romero. 2003. Marine *Cocconeis* Ehrenberg (Bacillariophyceae) species and related taxa from Kerguelen's Land (Austral Ocean, Indian Sector). Bibliotheca Diatomologica Band 47. J. Cramer, Berlin, p. 189.

Riaux-Gobin, C., A. Witkowski, J.P. Kociolek, L. Ector, D. Chevallier, and P. Compère. 2017. New epizoic diatom (Bacillariophyta) species from sea turtles in the Eastern Caribbean and South Pacific. Diatom Research 32: 109–125.

Round, F.E., R.M. Crawford, and D.G. Mann. 1990. The diatoms. Biology and morphology of the genera. Cambridge University Press, Cambridge, p. 747.

Rosel, P.E., L.A. Wilcox, T.K. Yamada, and K.D. Mullin. 2021. A new species of baleen whale (Balaenoptera) from the Gulf of Mexico, with a review of its geographic distribution. Marine Mammal Science 37: 577–610.

Ross, R., and P.A. Sims. 1972. The fine structure of the frustule in centric diatoms: a suggested terminology. British Phycological Journal 7: 139–163.

Stepanek J.G., and J.P. Kociolek. 2018. *Amphora* and *Halamphora* from inland waters of the United States and Japan, with the description of 33 new species. Bibliotheca Diatomologica 66, J. Cramer, Stuttgart, p.260.

Stepanek J.G., and J.P. Kociolek. 2019. Molecular phylogeny of the diatom genera *Amphora* and *Halamphora* (Bacillariophyta) with a focus on morphological and ecological evolution. Journal of Phycology 55: 442–456.

Stepanek J.G., T.E. Carlson, L.E. Rumley, and M.L. Julius. 2023. Systematic reappraisal of the diminutive *Amphora thumensis* and the transfer of *Halamphora parathumensis* to the genus *Amphora*. Diatom Research 38: 135–142.

Usachev, P.I. 1940. Der Diatomeenbewuchs auf Walen]. Zoologicheskii Zhurnal 19: 306-312. [In Russian.]

Wells, R.S., H.L. Rhinehart, L.J. Hansen, J.C. Sweeney, F.I. Townsend, et al. 2004. Bottlenose dolphins as marine ecosystem sentinels: Developing a health monitoring system. EcoHealth 1: 246–254.